NEW METHODS

Deciphering the Epigenetic Code of Cardiac Myocyte Transcription

Sebastian Preissl[1], Martin Schwaderer[1], Alexandra Raulf[2], Michael Hesse[2], Björn A. Grüning[3], Claudia Köbele[1], Rolf Backofen[3], Bernd K. Fleischmann[2,4], Lutz Hein[1,5], Ralf Gilsbach[1]

[1]Institute of Experimental and Clinical Pharmacology and Toxicology, University of Freiburg, Freiburg, Germany; [2]Institute of Physiology I, Life and Brain Center, University of Bonn, Bonn, Germany; [3]Bioinformatics Group, Department of Computer Science, University of Freiburg, Freiburg, Germany; [4]Pharma Center Bonn, Bonn, Germany, and; [5]BIOSS Centre for Biological Signaling Studies, University of Freiburg, Freiburg, Germany.

Running title: Methods to Study Cardiac Myocyte Epigenomics

Subject codes:
[142] Gene expression
[143] Gene regulation
[155] Physiological and pathological control of gene expression

Address correspondence to:

Dr. Ralf Gilsbach
Institute of Experimental and Clinical
Pharmacology and Toxicology
University of Freiburg
Albertstrasse 25
79104 Freiburg
Germany
Tel: +49-761-2035323
Fax: +49-761-2035318
ralf.gilsbach@pharmakol.uni-freiburg.de

Dr. Lutz Hein
Institute of Experimental and Clinical
Pharmacology and Toxicology
University of Freiburg
Albertstrasse 25
79104 Freiburg
Germany
Tel: +49-761-2035313
Fax: +49-761-2035318
lutz.hein@pharmakol.uni-freiburg.de

In May 2015, the average time from submission to first decision for all original research papers submitted to *Circulation Research* was 15.49 days.

ABSTRACT

Rationale: Epigenetic mechanisms are crucial for cell identity and transcriptional control. The heart consists of different cell types including cardiac myocytes, endothelial cells, fibroblasts and others. Therefore, cell type-specific analysis is needed to gain mechanistic insight into the regulation of gene expression in cardiac myocytes. While cytosolic mRNA represents steady-state levels, nuclear mRNA more closely reflects transcriptional activity. To unravel epigenetic mechanisms of transcriptional control, cell type-specific analysis of nuclear mRNA and epigenetic modifications is crucial.

Objective: The aim was to purify cardiac myocyte nuclei from hearts of different species by magnetic- or fluorescent-assisted sorting and to determine the nuclear and cellular RNA expression profiles and epigenetic marks in a cardiac myocyte-specific manner.

Methods and Results: Frozen cardiac tissue samples were used to isolate cardiac myocyte nuclei. High sorting purity was confirmed for cardiac myocyte nuclei isolated from mice, rats and humans. Deep sequencing of nuclear RNA revealed a major fraction of nascent, unspliced RNA in contrast to results obtained from purified cardiac myocytes. Cardiac myocyte nuclear and cellular RNA expression profiles showed differences especially for metabolic genes. Genome-wide maps of the transcriptional elongation mark H3K36me3 were generated by chromatin-immunoprecipitation. Transcriptome and epigenetic data confirmed the high degree of cardiac myocyte-specificity of our protocol. An integrative analysis of nuclear mRNA and histone mark occurrence indicated a major impact of the chromatin state on transcriptional activity in cardiac myocytes.

Conclusions: This study establishes cardiac myocyte-specific sorting of nuclei as a universal method to investigate epigenetic and transcriptional processes in cardiac myocytes of different origins. These data sets provide novel insight into cardiac myocyte transcription.

Nonstandard Abbreviations and Acronyms:

FACS	fluorescence-assisted nuclei sorting
FPKM	fragments per kilobase of exon per million mapped reads
kb	kilobase pair
MACS	magnetic-assisted nuclei sorting
nucRNA	nuclear mRNA
PCM1	pericentriolar material 1
RPKM	reads per kilobase per million mapped reads
TSS	transcription start site

INTRODUCTION

Precise spatio-temporal regulation of gene expression in cardiac myocytes is essential to meet the requirements during cardiac development as well as under pathophysiological conditions of the heart[1]. This requires adaptation of chromatin density by epigenetic processes like DNA methylation, histone modifications and ATP-dependent chromatin remodeling complexes[2]. Trimethylation of H3K4 as well as acetylation of H3K27 at promoter regions are linked to transcriptional activation, whereas DNA methylation and trimethylation of H3K27 at promoters and in gene bodies are associated with gene repression[3]. In addition, trimethylation of H3K36 is enriched at gene bodies of expressed genes linked to co-transcriptional splicing[4]. Cellular steady-state mRNA levels are affected by post-transcriptional splicing, polyadenylation or mRNA degradation[5]. All of these processes control the amount of mRNA available for protein translation. Therefore, analysis of nuclear unprocessed RNA is advisable to get direct insight into transcriptional activity[6] and its correlation with chromatin states. Most epigenetic studies in the heart focused on the analysis of cardiac tissue. Since cardiac myocyte nuclei represent only one third of cardiac nuclei in adult hearts and cell type composition changes during development of the heart and in disease[7], cardiac myocyte-specific maps of epigenetic modifications and nuclear transcriptome data are needed. Cardiac myocytes can be isolated by enzymatic digestion of cardiac tissue at physiological temperatures[8]. As this might alter chromatin states and transcriptional activity we developed protocols that do not involve enzymatic steps and are carried out under cold conditions to maintain the in vivo situation.

In the present study we demonstrate purification of cardiac myocyte nuclei from several species including human. This enabled us to generate cardiac myocyte-specific genome-wide maps of several histone modifications and nuclear transcriptomes. The high proportion of detected nascent unspliced RNA allows novel insight into transcriptional activity of cardiac myocytes. The nuclear transcript abundancies greatly differ from cellular levels in cardiac myocytes. In addition, gene transcription could be predicted by a model incorporating data of several key histone modifications. Our results open new possibilities to analyze epigenetic signatures and transcriptional activity of cardiac myocytes in development and disease.

METHODS

Animal procedures.
All animal procedures were approved by the responsible animal care committee (Regierungspräsidium Freiburg, Germany and Landesamt für Natur, Umwelt und Verbraucherschutz, Recklinghausen, Germany); these conformed to the Guide for the Care and Use of Laboratory Animals published by the National Academy of Sciences 2011. Twelve weeks old male C57BL/6N mice, twelve weeks old female Myh6-H2B-mCherry transgenic mice[9] and Wistar rats were used. Experimental infarction by ligation of the left anterior descending coronary artery was performed as described [9].

Human cardiac biopsies.
Left ventricular biopsies from hearts were used for cardiac myocyte nuclei isolation. These investigations were approved by the ethics committee of the University of Freiburg.

Immunohistochemistry.
Cryosections were stained with an antibody against PCM1[10] and a labeled secondary anti-rabbit antibody. Griffonia simplicifolia lectin I staining was used to visualize the glycocalyx of endothelial cells. Nuclei were stained with DAPI (4',6-diamidino-2-phenylindole) and Hoechst 33342 (Life technologies).

Isolation of cardiac nuclei.
Cardiac nuclei were isolated as described[7]. For the isolation of nuclear RNA, RNAsin (80 U/ml, Promega) was added to all buffers.

Magnetic-assisted sorting of cardiac myocyte nuclei.
For magnetic-assisted sorting, cardiac myocyte nuclei were incubated with an anti-PCM1 antibody[7] and sorting was performed as described[7].

Flow cytometric analysis and sorting of cardiac myocyte nuclei.
Cardiac myocyte nuclei were identified by an anti-PCM1 antibody. Nuclei were analyzed (CyFlow Space, Partec) or sorted (Bio-Rad S3, Bio-Rad) by flow cytometry.

ChIP-sequencing.
ChIP-seq was performed as described previously with modifications[7, 11]. Chromatin was precipitated with an anti-H3K36me3 antibody (1 µg, ab9050, Abcam) overnight. Data were deposited to the NCBI BioSample database (SRP033385).

Gene expression analysis.
Total RNA was isolated from cardiac myocyte nuclei or intact cardiac myocytes[7] derived from individual mouse hearts using RNeasy Micro Kit (Qiagen). RNA-seq libraries were generated from ribosomal depleted RNA and were sequenced on a HiSeq 2500 (50 bp, Illumina). Data were deposited to the NCBI BioSample database (SRP033386).

Bioinformatic analysis.
Sequencing reads were mapped to the *Mus musculus* genome (mm9) and duplicate reads were removed. Transcript abundance was calculated as fragments per kilobase of exon per million mapped reads (FPKM) and enrichment of histone modifications determined as reads per kilobase per million mapped reads (RPKM). The major isoform of each gene was used for all analysis steps. Quantified ChIP-seq reads were used to predict transcript levels. RPKM values of different histones were combined to increase the goodness of fit. Genomic regions enriched for histone modifications were identified by MACS2[12].

External data sets.
Previously published MethylC-seq data and ChIP-seq data (H3K27ac, H3K4me3, H3K4me1 and H3K27me3) from adult mouse cardiac myocyte nuclei were analyzed as described[7]. ChIP-seq data, MethylC-seq data and RNA-seq data were reanalyzed[13-16].

Gene ontology analysis.
Enriched GO terms of the category 'biological process' were identified by ClueGO[17].

RESULTS

Method outline.

We developed a protocol for the isolation of highly pure cardiac myocyte nuclei from small tissue biopsies (Figure 1). In contrast to traditional approaches involving enzymatic tissue dissociation to obtain cell suspensions[8], the described procedures do not involve enzymatic steps and are carried out under cold conditions to maintain the *in vivo* epigenetic state. Furthermore, our protocol enables characterization of frozen cardiac samples from experimental animal models as well as cardiac tissue biopsies from patients. Sorting relies either on fluorescence- (FACS) or magnetic-assisted nuclei sorting (MACS). As we have previously shown, these sorted nuclei were suitable for epigenetic analysis[7]. These procedures were optimized for genome-wide analysis of epigenetic marks in cardiac myocyte nuclei derived from small amounts of tissue (Online Table I). Furthermore, we established RNA sequencing of nuclear mRNA (nucRNA) to gain insight into transcriptional activity. To assess cellular steady-state RNA levels, we performed RNA sequencing from intact cardiac myocytes purified by FACS (Figure 1).

Staining of cardiac myocyte nuclei.

The basis of the presented method is the detection of pericentriolar material 1 (PCM1), a protein which in the heart is specifically bound to cardiac myocyte nuclei[7, 10]. To further prove the specificity of the peri-nuclear PCM1 staining in cardiac myocytes, we took advantage of a transgenic mouse model, in which a fusion protein of human histone H2B and mCherry (H2B-mCh) under control of the cardiac myocyte-specific *Myh6* promoter labels exclusively all cardiac myocyte nuclei[9]. We stained cryosections of left ventricles from these transgenic mice with an antibody against PCM1 (Figure 2A). Analysis of 10167 nuclei (n = 2 hearts) revealed a very high overlap of PCM1 and H2B-mCh signals (Figure 2A). PCM1 staining had a high specificity (>99.9%, i.e. only 1 false positive PCM1$^+$ nucleus out of 6499 H2B-mCh$^-$ nuclei) and sensitivity (99.9%, i.e. only 5 false negative PCM1$^-$ nuclei out of 3667 Hb2-mCh$^+$ nuclei) (Figure 2A). We also explored the cardiac myocyte-specific expression pattern in the scar area of infarcted hearts from H2B-mCh transgenic mice. Analysis of 4392 nuclei showed for 99.5% of the nuclei PCM1 and H2B-mCh signals (Figure 2B). Only negligible fractions of nuclei single positive for PCM1 (0.21 ± 0.1 % of nuclei) or for H2B-mCh (0.34 ± 0.2 %) were found (Figure 2B). Furthermore, we analyzed PCM1 staining in endothelial as well as smooth muscle cells. The glycocalyx of endothelial membranes was visualized by fluorescently labeled Griffonia simplicifolia lectin I[18] (GSL, Figure 2A, B), while smooth muscle cells were visualized by α-smooth muscle actin (ACTA2) staining (Online Figure II). Analysis of 309 α-smooth muscle actin positive cells did not reveal a single cell with perinuclear PCM1 staining (Online Figure II A, B). In addition, endothelial cells as identified by presence of GSL and absence of H2B-mCh signals did neither show PCM1 staining in native hearts nor in hearts after myocardial infarction (Online Figure IIC, D). 3 out of 1658 GSL positive cells were both H2B-mCh positive and PCM1 positive and thus could not be classified as cardiac myocytes or endothelial cells (Online Figure IIC, D). We also tested PCM1 specificity in single cardiac cells after Langendorff cell isolation (Figure 2C). Very similar, we did not detect PCM1 staining in non-cardiac myocytes (H2B-mCh negative and non-rod shaped, 0 out of 173, Figure 2C). All rod shaped cardiac myocytes were PCM1 and H2B-mCh positive. Some non-rod shaped cardiac myocytes (H2B-mCh positive) showed loss of the PCM1 signal, possibly due to cell death (Figure 2C).

Analysis and sorting of cardiac myocyte nuclei.

Flow cytometry experiments showed that PCM1 staining also labeled isolated nuclei (Figure 2D-F). To evaluate whether the protocol was applicable to different species, we also analyzed human and rat hearts in addition to mouse hearts. In all three species PCM1 staining of cardiac myocyte nuclei was evident (Figure 3A). Remarkably, the proportion of PCM1 positive nuclei detected in frozen and fresh

hearts was 99 ± 1.1 % (mean ± SEM, n =8) identical. Purification of cardiac myocyte nuclei by MACS was highly reproducible as assessed by flow cytometry (> 94 % purity, Figure 3B). These results highlight that PCM1 enables isolation of cardiac myocyte nuclei from hearts of different species including frozen clinical samples.

Nuclear RNA-seq of cardiac myocytes.

We chose mouse cardiac myocyte nuclei to generate transcriptomes by paired-end sequencing using a random priming strategy. From two independent experiments we generated sequencing libraries with mean insert sizes of 253 and 343 bp. We obtained 80 million uniquely mapped reads. For comparison, we assessed gene expression in intact cardiac myocytes by RNA-seq (cellular RNA-seq). Langendorff digestion was used to isolate cardiac cells. The obtained cell suspension contained 19 ± 4% non-cardiac myocytes (n = 4, mean ± SEM, Online Figure IA). Therefore, we further purified viable cardiac myocytes by FACS (Online Figure IB) and generated a library with a mean insert size of 312 bp and obtained 38 million uniquely mapped RNA-seq reads.

In contrast to cellular RNA-seq, nuclear RNA-seq showed high read coverage of intronic regions as illustrated in Figure 4A for the representative gene, phospholamban (*Pln*) (Figure 4A). Reads of cellular RNA-seq mapped predominantly into exonic regions of *Pln* (Figure 4A). However, nuclear RNA-seq data showed a large fraction of unspliced nascent *Pln* transcripts (Figure 4A). Based on intronic reads we calculated the fraction of unspliced mRNAs for all genes with high read coverage (> 10 FPKM) and exon-exon junctions. This global analysis revealed that 60.8% of nuclear mRNAs were unspliced. In intact cardiac myocytes, the unspliced fraction was only 2.6% (Figure 4B). These findings confirmed our hypothesis that nuclear mRNA analysis is less affected by posttranscriptional modifications and thus enables insight into transcriptional activity. Remarkably, nuclear RNA-seq showed a more than 4-fold higher fraction of reads uniquely mapping to non-coding RNA transcripts as compared to cellular RNA-seq (Figure 4C, Online Table II).

A drawback of nuclear RNA preparation is the likelihood of genomic DNA contamination. To quantify remaining DNA contamination we included two megabases of random sequences from the repeat-masked non-coding part of the genome in our bioinformatics analysis. In average, we detected 0.062 FPKM (0.049-0.074 FPKM, 95% confidence interval) in these regions. This value was regarded as the lower detection limit of our nuclear RNA-seq. 12,653 of 20,174 annotated coding genes showed transcriptional rates above this background (Figure 4D). Genes with the highest nuclear transcript levels were the cardiac myocyte genes troponin T type 2, α-myosin heavy chain, titin and myosin light-chain 2. Next we asked, whether nuclear and cellular mRNA profiles differ in cardiac myocytes. By visual inspection we identified natriuretic peptide A (*Nppa*) mRNA predominantly in the cellular RNA-seq (Figure 5A) whereas myosin heavy chain 7b (*Myh7b*) mRNA was mainly detected in nuclei (Figure 5B). In order to identify transcripts with the most differential abundance we calculated $\log_2$ ratios of FPKM values between cellular and nuclear mRNAs for transcripts with expression > 1 FPKM in cardiac myocyte nuclei (Figure 5C). Cellular to nuclear RNA expression ratios differed over several orders of magnitude (Figure 5C). Gene ontology analysis of RNAs that were primarily expressed in cells as compared to nuclei (> 95th percentile, Figure 5C) showed significant enrichment for genes involved in energy metabolism (Figure 5D). On the other hand, mRNAs with higher abundance in nuclei (< 5th percentile, Figure 5C) showed an overrepresentation of genes associated with transcriptional regulation (Figure 5E).

Cell-type specificity of epigenetic and transcriptome data obtained from PCM1-sorted nuclei.

The heart consists of many different cell types including cardiac myocytes, fibroblasts, endothelial cells, smooth muscle cells and others[19]. Analysis of cardiac tissue thus shows the overlay of epigenetic and transcriptome signatures of different cardiac cell-types. We postulated that data obtained from PCM1-sorted nuclei were highly cardiac myocyte-specific. We compared our data from PCM1-positive cardiac myocyte nuclei with previously published data sets from cardiac tissue biopsies (Figure 5A-D, Online Figure III)[14, 16, 20]. Figure 5 shows the results of the representative cardiac myocyte-specific gene myosin light chain 3 (*Myl3*) and the mesenchymal non-cardiac myocyte gene vimentin (*Vim*)[21]. In cardiac myocyte nuclei, the promoter region of *Myl3* was enriched for acetylation of lysine 27 of histone 3 (H3K27ac, Figure 6A). Acetylation of H3K27 is an epigenetic hallmark of active genomic regions[22]. In contrast, no H3K27ac signal could be detected in the promoter region of *Vim* in cardiac myocyte nuclei (Figure 6B). On the other hand, the *Vim* promoter was enriched for trimethylated H3K27, a mark that is considered to be an indicator of gene silencing[23] (Figure 6B). This repressive mark was absent in the promoter region of *Myl3* in cardiac myocyte nuclei (Figure 6A). These results were in line with RNA-seq data revealing that *Myl3* but not *Vim* was expressed in cardiac myocyte nuclei (Figure 6A, B). Analysis of heart tissue showed gene expression of both genes and a mixture of active and inactive histone marks (Figure 6C, D). In addition, CpG methylation profiles of cardiac myocytes showed a clear topology as compared to profiles obtained from cardiac tissue biopsies (Figure 6A-D). Previously reported cardiac myocyte-specific demethylation of the genic region of *Myl3*[7] was only visible in cardiac myocyte nuclei but not in total heart samples (Figure 6A, C). The obtained results were further validated by analysis of the endothelial cell gene angiotensin-converting enzyme (*Ace*)[24] and the fibroblast gene collagen alpha-2(I) chain (*Col1a2*)[25] (Online Figure III). We compared our ChIP-seq data with data derived from *in-vitro* differentiated cardiac myocytes[13] to confirm validity. Similar enrichment profiles of histone modifications were observed for representative cardiac myocyte genes as well as for averages of genes grouped according to quantiles of expression in cardiac myocyte nuclei (Online Figure IV). Differences were observed regarding non-cardiac myocyte marker genes and histone peaks adjacent to developmental genes (Online Figure IV).

We asked which gene promoters were active according to acetylation of H3K27 in cardiac myocyte nuclei and in cardiac tissue. Therefore, we identified all promoters overlapping with an H3K27ac peak in hearts and in cardiac myocyte nuclei, respectively. We could identify 10,123 active promoters in hearts (Figure 7A, C). 936 of these lacked H3K27ac in cardiac myocyte nuclei, indicating that they were not active in cardiac myocytes but in other cardiac cell types (Figure 7A,C, black section). Gene ontology classification of H3K27ac ChIP-seq peaks detected in heart tissue but not in cardiac myocyte nuclei (Figure 7C) showed association with extracellular matrix organization, vascular development, regulation of immune system processes and cell migration (p < 10^{-10}, Figure 7B). This suggests that these H3K27ac signals originate from cardiac fibroblasts, endothelial cells or immune cells but not from cardiac myocytes. Analysis of these promoter regions showed enrichment for H3K27me3 in hearts as well as in cardiac myocyte nuclei (Figure 7D). Promoters active in hearts and cardiac myocytes (Figure 7D, grey box) were depleted for H3K27me3 in cardiac myocytes. In contrast, results obtained from hearts showed enrichment for H3K27me3, probably due to silencing of these genes in non-cardiac myocytes (Figure 7D, grey box).

Histone marks are predictive for transcription in cardiac myocytes.

We extended the analysis to further histone marks to get a more detailed picture. Previous studies showed that H3K36me3 is tightly linked to active transcription and peaks in gene bodies of active genes[11, 26]. We performed ChIP-seq experiments for the histone mark H3K36me3 in purified cardiac myocyte nuclei. We generated 22 million uniquely mapped readscing. In addition, we reanalyzed our previously published ChIP-seq data and asked which epigenetic marks were most predictive for cardiac myocyte transcription.

The tropomyosin 1 gene (*Tpm1*) encodes for a protein of the contractile apparatus[27]. It showed the typical epigenetic signature of a highly expressed gene (Figure 8). Several isoforms of *Tpm1* are annotated (Online Figure V). Previous studies have shown that *Tpm1* isoforms are expressed in different cell-types[27]. For a proper analysis of the interplay of chromatin features and RNA transcription it is crucial to identify the expressed isoform(s). We used nuclear RNA-seq reads from the spliced fraction to determine genome-wide exon-exon junctions and selected the main cardiac myocyte isoform of each gene for further analysis steps. In cardiac myocyte nuclei, only one *Tpm1* isoform was detected (transcript 8, Online Figure V). This cardiac myocyte isoform of *Tpm1* was concordant with epigenetic patterns of the *Tpm1* gene. The region around the annotated transcription start site was decorated with H3K27ac. We observed strong enrichment of H3K36me3 in exonic regions of *Tpm1* (Figure 7A, Online Figure V). During transcription RNA polymerase II interacts with SETD2 (SET domain containing 2)[28] resulting in trimethylation of H3K36. Previous studies linked exon marking by H3K36me3 to splicing activity during active transcription[4, 29]. In contrast, H3K4me3 is enriched at active promoters and promoters with high CpG density[30]. For *Tpm1* two different transcription start sites are annotated (Online Figure V). Both overlap with regions of high CpG density (CpG islands) and thus were marked by H3K4me3 (Online Figure IV). Only the cardiac myocyte-specific transcription start region was enriched for H3K27ac, too (Figure 8A, Online Figure V). The H3K4me3 mark was strongly enriched at the 5' region of the *Tpm1* gene, whereas the remainder of the gene body was decorated by H3K4me1 (Figure 8A, Online Figure V). This showed the mutually exclusive nature of H3K4me1 and H3K4me3[28] in purified nuclei. The repressive histone mark H3K27me3 was absent at the entire *Tpm1* locus (Figure 8A, Online Figure V). In a previous study we showed that low levels of gene body CpG methylation were characteristic for highly expressed cardiac myocyte genes[7]. In agreement with these results, large domains of the gene body of *Tpm1* showed strong demethylation of CpGs with lowest levels of DNA methylation in the 5´-region (Online Figure V). These data demonstrate that specific histone patterns mark expression of gene isoforms in cardiac myocytes.

In order to correlate transcript levels with histone marks, the genomic regions decorated by specific histone marks in cardiac myocyte nuclei were identified. Coding genes showed a clear pattern with marking of promoters of expressed genes by H3K27ac and H3K4me3 and of gene bodies by H3K4me1 and H3K36me3 (Online Figure VI). Furthermore genes lacking these marks were marked by H3K27me3 in genic regions (Online Figure VI). These genomic locations were selected for quantitative analysis.

To test if histone marks are predictive for nuclear mRNA expression we ranked all coding genes according to expression level. Genes not expressed in cardiac myocyte nuclei (< 0.062 FPKM, gene expression rank > 12,653) showed high H3K27me3 enrichment (Figure 8B). These genes were depleted for the active marks H3K4me3, H3K4me1, H3K36me3 and H3K27ac. Expressed genes gained active histone marks concordant with expression levels and lost H3K27me3 (Figure 8B).

These data prompted us to analyze the predictive information of the individual marks for transcriptional activity. Linear modeling of transcription from individual histone marks showed a significant positive correlation with measured nucRNA levels in case of H3K4me1, H3K4me3, H3K27ac and H3K36me3 (p < 0.001, Figure 8C). A negative correlation with gene expression was observed for H3K27me3 (p < 0.001). H3K27ac contained the highest predictive information for a single histone mark. 70% of nucRNA expression differences could be explained by enrichment of H3K27ac at promoter regions (Figure 8C). The predictive power of the model was further improved to 78% by addition of results from assessed histone marks (Figure 8C, D). A scatter plot of predicted and measured nuclear RNA showed a large overlap for expressed as well as not-expressed genes. A linear correlation of gene expression values obtained from this prediction with cellular and heart RNA-seq data (Online Figure VII) yielded 74% and 71% (Online Figure VII), respectively. Remarkably, the prediction was especially weaker in case of expressed genes. This was even more evident in case of non-cardiac data sets[20] further reducing the strength of correlation to 39-42% (Online Figure VII).

DISCUSSION

We provide detailed methods for the in depth analysis of epigenetic modifications in cardiac myocytes. Furthermore, we present - for the first time - a technique to study nascent RNA transcripts of cardiac myocytes. Fresh as well as frozen cardiac tissue from different species including human can be purified using our workflow.

To date most epigenetic and transcriptome studies in cardiovascular research have analyzed cardiac tissue biopsies[31]. Epigenetic and gene expression signatures are highly cell type-specific[32]. Therefore, analysis of tissues consisting of complex cell type mixtures may lead to ambiguous results. Indeed, changes in cellular composition itself may lead to varying results[32]. This point should not be neglected in heart research, since several conditions are known to affect the cellular composition of the heart. For example, pathophysiological conditions like cardiac pressure overload or myocardial infarction induce cellular changes as part of cardiac remodeling[33, 34]. These changes involve apoptosis of cardiac myocytes, proliferation of fibroblasts and endothelial cells as well as invasion of inflammatory cells.

The importance to consider these alterations is highlighted by a recent manuscript reanalyzing previously published data sets of age-associated epigenetic changes in the blood. Most of the observed variability could be explained simply by cellular composition[35]. Our recent findings support the significance of altered cellular composition for cardiac epigenetic studies[7]. Significant differences of CpG methylation levels in biopsies of hypertrophic and healthy hearts were caused by disease-associated loss of cardiac myocytes and increased abundance of fibroblasts and other non-cardiac myocyte cells[7]. Analysis of complex tissues like hearts may also lead to misinterpretation of chromatin signatures. Coexistence of repressive and active marks on the same allele has been observed in cell types with restricted differentiation potency or pluripotency[36]. Remarkably, this bivalency could not be observed in our datasets of adult cardiac myocytes. ChiP-seq data from hearts resemble the picture of bivalency, but it is very likely that the signals of the active and inactive marks originate from different cell-types.

These facts underscore the need for cell type-specific studies. To meet this demand we developed methods for the epigenetic and transcriptome analysis of purified cardiac myocyte nuclei. We and others reported PCM1 as a marker of cardiac myocyte nuclei in different species[7, 10]. In the present manuscript, different immunohistochemistry quantification strategies in healthy, transgenic and diseased hearts show that > 98 % of cardiac myocyte nuclei are positive for PCM1. These results are in very good agreement with our previously reported FACS data[7]. Furthermore, the specificity of PCM1 has recently been

reported for human cardiac myocytes[37]. Our whole genome data of nuclear mRNA expression and epigenetic marks further support the validity of PCM1 as a cardiac myocyte-specific marker.

In contrast to traditional approaches involving enzymatic tissue dissociation to obtain cell suspensions[8], the described procedures do not involve enzymatic steps and are carried out under cold conditions to maintain the *in vivo* epigenetic state. Our method is applicable to different developmental and disease stages of several species including frozen clinical samples without protocol modifications.

The initial step of the workflow is disruption of cardiac biopsies and purification of nuclei. The described tissue disruption and purification procedures ensure efficient and reliable isolation of nuclei from frozen as well as fresh cardiac biopsies. Isolated nuclei can be sorted by FACS. In addition, we established magnetic-assisted sorting of antibody-labeled nuclei (MACS) which enables processing of samples in parallel. Both methods yielded highly pure preparations.

To date several studies performed deep sequencing of the cardiac transcriptome[38, 39]. In the present manuscript, we studied for the first time the nuclear transcriptome of cardiac myocytes. In comparison to cellular RNA, nucRNA represents freshly transcribed (nascent) mRNA and therefore correlates more closely with transcriptional activity. The validity of this assumption was proven by the large fraction of detected unspliced mRNAs and is in good agreement with previous reports assessing nucRNA in other cell-types[6, 40]. Our data sets enabled us for the first time to identify the entire set of genes transcribed in cardiac myocytes. Epigenetic data confirmed these results since transcribed genes showed an epigenetic signature distinct from non-expressed genes.

Following transcription, several mechanisms modulate mRNA abundance. Comparing nuclear and cellular mRNA levels in cardiac myocytes revealed distinct patterns of expression. Remarkably, a large fraction of metabolic genes seems to accumulate in the cytosol. Several mechanisms could account for these differences including post-transcriptional processing, mRNA decay and miRNA mediated degradation[5, 11, 41].

Next, we proposed a model to deduce quantitatively nuclear transcript levels from epigenetic data. The highest informative value among the assessed histone modifications had H3K27ac. To improve the accuracy of the model, we combined the results of five key histone marks. This model explained 78% of gene expression alteration by epigenetic marks. Comparable results have been obtained in different cell lines [11, 42, 43]. A cross-comparison of the predictive model of cardiac myocyte gene expression with measured RNA levels in non-cardiac tissues showed a weak correlation (Online Figure VII). This underscores that the chromatin state of promoter and genic regions is a major determinant of cell-type specific transcriptional activity. Factors explaining the remaining transcriptional variability include varying activity of enhancers[44] and transcription factors[45]. This tight link of chromatin state and transcriptional activity can only be uncovered in cell-type specific data sets.

Nuclei purified with the proposed protocol are principally suitable to study other nuclear processes in cardiac myocytes. The proposed protocol opens new possibilities to study gene transcription and epigenetic mechanisms in cardiac myocytes from different species and developmental stages including clinical samples. This will be of great value to pave the way to a better understanding of cardiac myocyte transcription in development and disease.

DISCLOSURES

None.

REFERENCES

1. Chang CP, Bruneau BG. Epigenetics and cardiovascular development. *Annu Rev Physiol*. 2012;74:41-68.
2. Nührenberg T, Gilsbach R, Preissl S, Schnick T, Hein L. Epigenetics in cardiac development, function, and disease. *Cell Tissue Res*. 2014;356:585-600.
3. Kouzarides T. Chromatin modifications and their function. *Cell*. 2007;128:693-705.
4. de Almeida SF, Grosso AR, Koch F, Fenouil R, Carvalho S, Andrade J, Levezinho H, Gut M, Eick D, Gut I, Andrau JC, Ferrier P, Carmo-Fonseca M. Splicing enhances recruitment of methyltransferase HYPB/Setd2 and methylation of histone H3 Lys36. *Nat Struct Mol Biol*. 2011;18:977-983.
5. de Klerk E, t Hoen PA. Alternative mRNA transcription, processing, and translation: insights from RNA sequencing. *Trends Genet*. 2015;31:128-139.
6. Mitchell JA, Clay I, Umlauf D, Chen CY, Moir CA, Eskiw CH, Schoenfelder S, Chakalova L, Nagano T, Fraser P. Nuclear RNA sequencing of the mouse erythroid cell transcriptome. *PLoS One*. 2012;7:e49274.
7. Gilsbach R, Preissl S, Grüning BA, Schnick T, Burger L, Benes V, Würch A, Bönisch U, Günther S, Backofen R, Fleischmann BK, Schübeler D, Hein L. Dynamic DNA methylation orchestrates cardiac myocyte development, maturation and disease. *Nat Commun*. 2014;5:5288.
8. O'Connell TD, Rodrigo MC, Simpson PC. Isolation and culture of adult mouse cardiac myocytes. *Methods Mol Biol*. 2007;357:271-296.
9. Raulf A, Horder H, Tarnawski L, Geisen C, Ottersbach A, Roll W, Jovinge S, Fleischmann BK, Hesse M. Transgenic systems for unequivocal identification of cardiac myocyte nuclei and analysis of cardiac myocyte cell cycle status. *Basic Res Cardiol*. 2015;110:489.
10. Bergmann O, Zdunek S, Alkass K, Druid H, Bernard S, Frisén J. Identification of cardiac myocyte nuclei and assessment of ploidy for the analysis of cell turnover. *Exp Cell Res*. 2011;317:188-194.
11. Tippmann SC, Ivanek R, Gaidatzis D, Scholer A, Hoerner L, van Nimwegen E, Stadler PF, Stadler MB, Schübeler D. Chromatin measurements reveal contributions of synthesis and decay to steady-state mRNA levels. *Mol Syst Biol*. 2012;8:593.

DOI: 10.1161/CIRCRESAHA.115.306337   11

12. Zhang Y, Liu T, Meyer CA, Eeckhoute J, Johnson DS, Bernstein BE, Nusbaum C, Myers RM, Brown M, Li W, Liu XS. Model-based analysis of ChIP-Seq (MACS). *Genome Biol*. 2008;9:R137.

13. Wamstad JA, Alexander JM, Truty RM, et al. Dynamic and coordinated epigenetic regulation of developmental transitions in the cardiac lineage. *Cell*. 2012;151:206-220.

14. Shen Y, Yue F, McCleary DF, Ye Z, Edsall L, Kuan S, Wagner U, Dixon J, Lee L, Lobanenkov VV, Ren B. A map of the cis-regulatory sequences in the mouse genome. *Nature*. 2012;488:116-120.

15. Consortium EP. An integrated encyclopedia of DNA elements in the human genome. *Nature*. 2012;489:57-74. Data set SRX185852 (Bing Ren lab, Ludwig Institue for Cancer Research) and data sets from study SRP012040 (Thomas Gingeras lab - Cold Spring Harbor Laboratory).

16. Hon GC, Rajagopal N, Shen Y, McCleary DF, Yue F, Dang MD, Ren B. Epigenetic memory at embryonic enhancers identified in DNA methylation maps from adult mouse tissues. *Nat Genet*. 2013;45:1198-1206.

17. Bindea G, Mlecnik B, Hackl H, Charoentong P, Tosolini M, Kirilovsky A, Fridman WH, Pages F, Trajanoski Z, Galon J. ClueGO: a Cytoscape plug-in to decipher functionally grouped gene ontology and pathway annotation networks. *Bioinformatics*. 2009;25:1091-1093.

18. Laitinen L. Griffonia simplicifolia lectins bind specifically to endothelial cells and some epithelial cells in mouse tissues. *Histochem J*. 1987;19:225-234.

19. Xin M, Olson EN, Bassel-Duby R. Mending broken hearts: cardiac development as a basis for adult heart regeneration and repair. *Nat Rev Mol Cell Biol*. 2013;14:529-541.

20. Consortium EP. An integrated encyclopedia of DNA elements in the human genome. *Nature*. 2012;489:57-74. Data sets from study SRP012040 (Thomas Gingeras lab - Cold Spring Harbor Laboratory).

21. Speiser B, Weihrauch D, Riess CF, Schaper J. The extracellular matrix in human cardiac tissue. Part II: Vimentin, laminin, and fibronectin. *Cardioscience*. 1992;3:41-49.

22. Carone BR, Rando OJ. Rewriting the epigenome. *Cell*. 2012;149:1422-1423.

23. Margueron R and Reinberg D. The Polycomb complex PRC2 and its mark in life. *Nature*. 2011;469:343-349.

24. Budden DM, Hurley DG, Cursons J, Markham JF, Davis MJ, Crampin EJ. Predicting expression: the complementary power of histone modification and transcription factor binding data. *Epigenetics Chromatin*. 2014;7:36.

25. Kumar V, Muratani M, Rayan NA, Kraus P, Lufkin T, Ng HH, Prabhakar S. Uniform, optimal signal processing of mapped deep-sequencing data. *Nat Biotechnol*. 2013;31:615-622.

26. Sims RJ, Reinberg D. Processing the H3K36me3 signature. *Nat Genet*. 2009;41:270-271.

27. Gunning PW, Schevzov G, Kee AJ, Hardeman EC. Tropomyosin isoforms: divining rods for actin cytoskeleton function. *Trends Cell Biol*. 2005;15:333-341.

28. Henikoff S, Shilatifard A. Histone modification: cause or cog? *Trends Genet*. 2011;27:389-396.

29. Kolasinska-Zwierz P, Down T, Latorre I, Liu T, Liu XS, Ahringer J. Differential chromatin marking of introns and expressed exons by H3K36me3. *Nat Genet*. 2009;41:376-381.

30. Lenhard B, Sandelin A, Carninci P. Metazoan promoters: emerging characteristics and insights into transcriptional regulation. *Nat Rev Genet*. 2012;13:233-245.

31. Di Salvo TG, Haldar SM. Epigenetic mechanisms in heart failure pathogenesis. *Circ Heart Fail*. 2014;7:850-863.

32. Michels KB, Binder AM, Dedeurwaerder S, Epstein CB, Greally JM, Gut I, Houseman EA, Izzi B, Kelsey KT, Meissner A, Milosavljevic A, Siegmund KD, Bock C, Irizarry RA. Recommendations for the design and analysis of epigenome-wide association studies. *Nat Methods*. 2013;10:949-955.

33. Kehat I, Molkentin JD. Molecular pathways underlying cardiac remodeling during pathophysiological stimulation. *Circulation*. 2010;122:2727-2735.

34. Cohn JN, Ferrari R, Sharpe N. Cardiac remodeling - concepts and clinical implications: a consensus paper from an international forum on cardiac remodeling. Behalf of an International Forum on Cardiac Remodeling. *J Am Coll Cardiol*. 2000;35:569-582.

35. Jaffe AE, Irizarry RA. Accounting for cellular heterogeneity is critical in epigenome-wide association studies. *Genome Biol*. 2014;15:R31.

36. Voigt P, Tee WW, Reinberg D. A double take on bivalent promoters. *Genes Dev*. 2013;27:1318-1338.

37. Bergmann O, Zdunek S, Felker A, et al. Dynamics of cell generation and turnover in the human heart. *Cell*. 2015;161:1566-1575.

38. Lee JH, Gao C, Peng G, Greer C, Ren S, Wang Y, Xiao X. Analysis of transcriptome complexity through RNA sequencing in normal and failing murine hearts. *Circ Res*. 2011;109:1332-1341.

39. Yang KC, Yamada KA, Patel AY, Topkara VK, George I, Cheema FH, Ewald GA, Mann DL, Nerbonne JM. Deep RNA sequencing reveals dynamic regulation of myocardial noncoding RNAs in failing human heart and remodeling with mechanical circulatory support. *Circulation*. 2014;129:1009-1021.

40. Zaghlool A, Ameur A, Nyberg L, Halvardson J, Grabherr M, Cavelier L, Feuk L. Efficient cellular fractionation improves RNA sequencing analysis of mature and nascent transcripts from human tissues. *BMC Biotechnol*. 2013;13:99.

41. Grueter CE, van Rooij E, Johnson BA, DeLeon SM, Sutherland LB, Qi X, Gautron L, Elmquist JK, Bassel-Duby R, Olson EN. A cardiac microRNA governs systemic energy homeostasis by regulation of MED13. *Cell*. 2012;149:671-683.

42. Karlic R, Chung HR, Lasserre J, Vlahovicek K, Vingron M. Histone modification levels are predictive for gene expression. *Proc Natl Acad Sci U S A*. 2010;107:2926-2931.

43. Dong X, Greven MC, Kundaje A, Djebali S, Brown JB, Cheng C, Gingeras TR, Gerstein M, Guigo R, Birney E, Weng Z. Modeling gene expression using chromatin features in various cellular contexts. *Genome Biol*. 2012;13:R53.

44. Wamstad JA, Wang X, Demuren OO, Boyer LA. Distal enhancers: new insights into heart development and disease. *Trends Cell Biol*. 2014;24:294-302.

45. Paige SL, Plonowska K, Xu A, Wu SM. Molecular regulation of cardiac myocyte differentiation. *Circ Res*. 2015;116:341-353.

ONLINE FIRST

FIGURE LEGENDS

Figure 1: Flow diagram of the protocol. Workflow for epigenetic and nuclear transcriptome analysis of cardiac myocyte nuclei isolated by fluorescent antibodies or magnetic antibodies (**A**). Intact cardiac myocytes were purified by FACS from cardiac single-cell suspensions for cellular transcriptome analysis (**B**).

Figure 2: Identification of cardiac myocyte nuclei by PCM1 staining.
A, B PCM1 staining in cryosections of a native adult Myh6-H2B-mCh transgenic heart (**A**, upper panel) and of an infarcted adult Myh6-H2B-mCh transgenic heart (**B**, upper panel). Dotted line separates scar region (upper) from border zone (lower part). Endothelial cells were identified by GSL (Griffonia simplicifolia lectin I) staining (quantitative results see Online Figure II) and nuclei by Hoechst 33342. Cross striation of cardiac myocytes is visible in differential interference contrast (DIC) (scale bars: 50 μm in overviews, 20 μm in close-up). **A** (lower panel) Quantification of PCM1 staining and H2B-mCh expression in cryosections of native adult Myh6-H2B-mCh transgenic hearts (n = 2 hearts, numbers indicate total counted nuclei). **B** (lower panel) Quantification of PCM1 staining and H2B-mCh expression in the border zone of infarcted adult Myh6-H2B-mCh transgenic hearts (d10 after left coronary artery ligation) (n = 2 hearts, numbers indicate total counted nuclei). **C** (upper panel) Langendorff isolated ventricular cardiac myocytes of adult Myh6-H2B-mCh transgenic hearts stained for PCM1 and α-actinin (α-ACT). Nuclei were visualized with Hoechst 33342. Insert shows PCM1 staining only (scale bars: 20 μm). **C** (lower panel) Quantification of PCM1 staining and H2B-mCh expression in Langendorff isolated cardiac cells of native adult Myh6-H2B-mCh transgenic hearts (n = 4, numbers indicate total counted cells). **D-F** Nuclei from mouse hearts were analyzed by flow cytometry. **D** Dot plot illustrating the identification of nuclei according to DAPI staining (black box). **E** Nuclei were treated with an IgG-isotype antibody and a corresponding secondary antibody. **F** Anti-PCM1 antibody and a corresponding secondary antibody stained cardiac myocyte nuclei (red color).

Figure 3: Analysis of hearts and sorting of cardiac myocyte nuclei from different species.
A Representative histograms and quantification of the proportion of cardiac myocyte nuclei in ventricles from mice, rats and humans (n = 5-7). **B** Representative histograms and quantification of sorting purity by MACS (n = 2-7).

Figure 4: Cardiac myocyte-specific deep sequencing of cellular vs. nuclear mRNA.
A Read coverage of phospholamban (*Pln*). **B** Genome wide analysis of coding mRNAs revealed predominance of unspliced transcripts in cardiac myocyte nuclei (*** p < 0.001, Student's *t*-test). **C** RNA-seq reads mapped to different RNA classes (nc, non-coding; m, messenger). **D** Pie chart of coding transcript expression in cardiac myocyte nuclei (FPKM: fragments per kilobase of exon per million mapped reads; RPKM: reads per kilobase per million mapped reads).

Figure 5: Comparison between nuclear RNA-seq and cellular RNA-seq data.
A, B Exemplary IGV traces of natriuretic peptide A (*Nppa*, **A**) and myosin heavy chain 7b (*Myh7b*, **B**) derived from cellular RNA-seq and nuclear RNA-seq. **C** Box plot with whiskers of mRNA ratios between nuclei and cells. Values below the 5th and greater than the 95th percentile are depicted as dots. **D** Gene ontology analysis of genes with higher cellular as compared to nuclear mRNA levels (greater than the 95th percentile). **E** Gene ontology analysis of genes with higher nuclear as compared to cellular mRNA levels (below the 5th percentile). **D, E** All significant terms are shown. (RPKM: reads per kilobase per million mapped reads, FPKM: fragments per kilobase of exon per million mapped reads).

Figure 6: Illustration of representative genomic regions underpinning the applicability of PCM1-sorted cardiac myocyte nuclei for transcriptome and epigenetic analysis.

A-D Exemplary traces illustrating mRNA expression, histone marks and DNA methylation maps for a cardiac myocyte gene, myosin light chain 3 (*Myl3*, **A**, **C**) and a non-myocyte gene, vimentin (*Vim*, **B**, **D**). In cardiac myocyte nuclei (**A**, **B**), the active histone mark H3K27ac was enriched at the *Myl3* locus (**A**), but not at the *Vim* gene (**B**). In cardiac myocyte nuclei *Vim* is decorated by the inactive histone mark H3K27me3 (**B**). In hearts, *Myl3* and *Vim* contained mixtures of H3K27ac and H3K27me3 marks (**C**, **D**). Specific patterns of genic DNA methylation (5m-CpG) were detectable in purified cardiac myocyte nuclei (**A**, **B**) but not in hearts (**C**, **D**; RPKM: reads per kilobase per million mapped reads).

Figure 7: Comparison of ChIP-seq data from hearts and cardiac myocyte nuclei.

A Pie chart illustrating the number of promoter regions (TSS ± 2 kb) overlapping with H3K27ac peaks in hearts and cardiac myocyte nuclei. **B** GO-classification of heart-specific H3K27ac positive promoters (Benjamini adjusted p-value < 10^{-10}). **C**, **D** Heat maps showing input-normalized enrichments for H3K27ac (**C**) and H3K27me3 (**D**) surrounding promoter sequences in hearts and cardiac myocyte nuclei. Shown are promoters overlapping with an H3K27ac peaks in in cardiac myocytes and/ or hearts. (RPKM: reads per kilobase per million mapped reads; TSS: transcription start site).

Figure 8: Histone modification profiles in cardiac myocytes were used to model gene expression in cardiac myocyte nuclei.

A Traces of nuclear mRNA expression and histone marks at the tropomyosin 1 locus (*Tpm1*) are depicted. Arcs represent reads mapped to exon-exon junctions. **B-D** Shown are results for the main isoform of coding genes (FPKM: fragments per kilobase of exon per million mapped reads; RPKM: reads per kilobase per million mapped reads; CI: confidence interval). **B** Enrichments of histone marks in the promoter region (H3K27ac, H3K4me3) or the gene body (H3K36me3, H3K4me1, H3K27me3) was dependent on gene expression in cardiac myocyte nuclei. Dashed lines represent the mean detection level of gene expression ± 95 % confidence interval. Genes were ranked according to expression levels. **C** Determination coefficients (r^2) of enrichments of different histone marks, nuclear mRNA expression and a linear model including different combinations of histone marks were calculated (* indicates inverse correlation). **D** Scatter plot of modeled gene expression calculated from patterns of different histone modifications using a linear model and measured nuclear mRNA expression (p < 0.0001). Colors represent densities of values. Regions were marked by darkblue, light blue, yellow, red and darkred in order of increasing densities.

Novelty and Significance

What Is Known?

- The cellular composition of the heart is changing during development and disease.

- Control of gene expression is essential for proper function of cardiac myocytes.

- Epigenetic control of transcription is highly cell-type specific.

What New Information Does This Article Contribute?

- This study provides a method for purification of cardiac myocyte nuclei from frozen heart tissue of several species.

- We have identified and quantified mRNAs transcribed in cardiac myocytes on the nuclear and cellular level.

- Chromatin state is a main predictor of transcriptional activity in cardiac myocytes.

Regulation of gene expression involves several processes including epigenetic control of transcriptional activity. However, the precise molecular mechanisms in cardiac myocytes in vivo are unknown. Thus, the aim of the present study was to establish epigenetic and transcriptomic profiling of purified cardiac myocyte nuclei from heart tissue. Cardiac myocyte nuclei were identified upon staining with an antibody against PCM1. Extensive validation demonstrated very high degrees of specificity and sensitivity of PCM1 staining for cardiac myocyte nuclei. Using this technique we identified RNA transcripts expressed in cardiac myocyte nuclei in vivo. A quantitative analysis of five histone marks was performed in order to define the chromatin state of cardiac myocyte genes. Chromatin status correlated significantly better with nuclear RNA than cellular RNA profiles. This integrative analysis indicated a major impact of the chromatin state on transcriptional activity in cardiac myocytes. Thus, cardiac myocyte-specific sorting of nuclei is a reliable method to investigate epigenetic and transcriptional processes in cardiac myocytes. The findings may open new mechanistic insight into the interplay of epigenetic mechanisms and transcription in cardiac myocytes during development and under pathophysiological conditions.

FIGURE 1

A Isolation of cardiac nuclei

Staining

Sorting

FACS

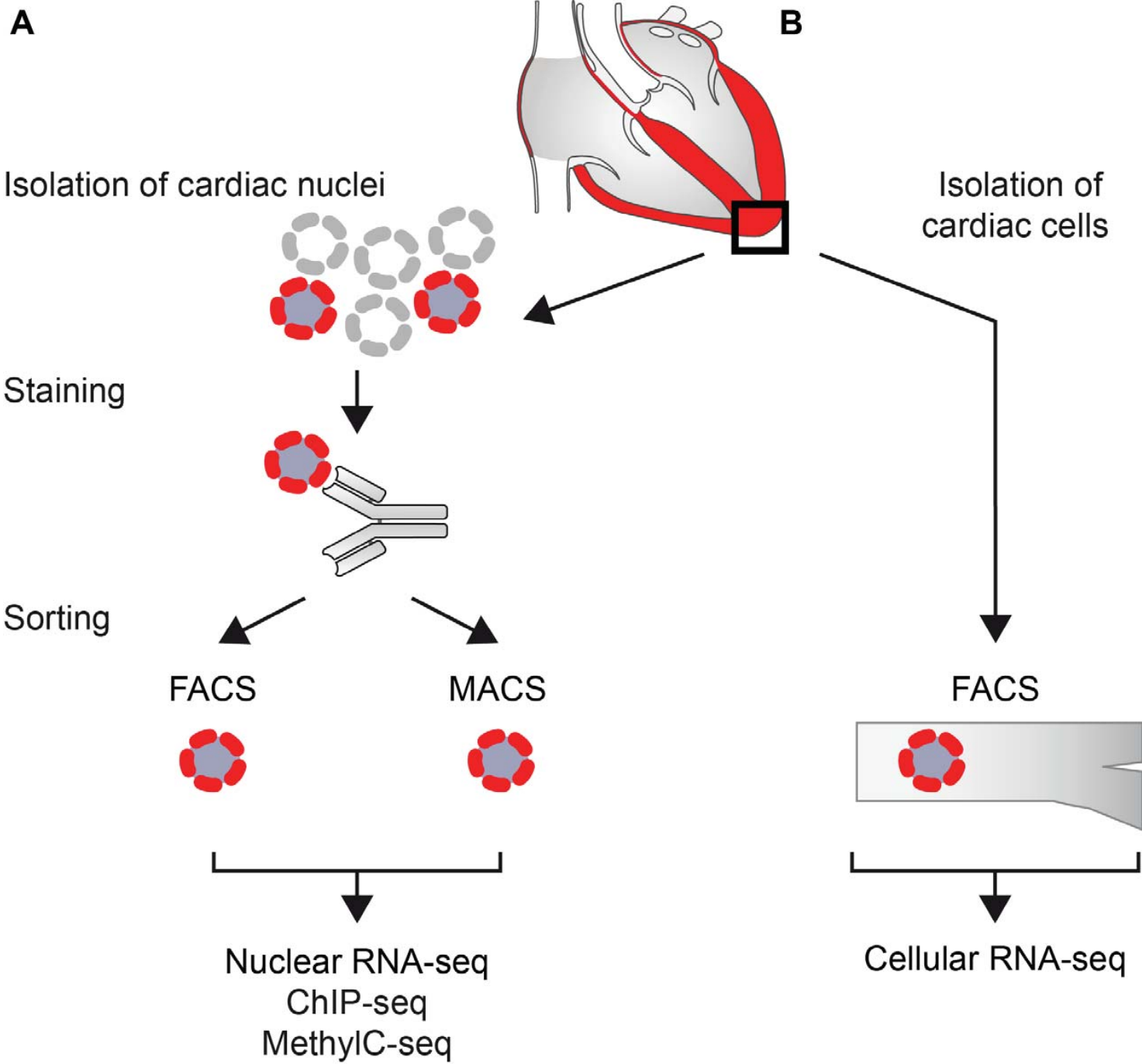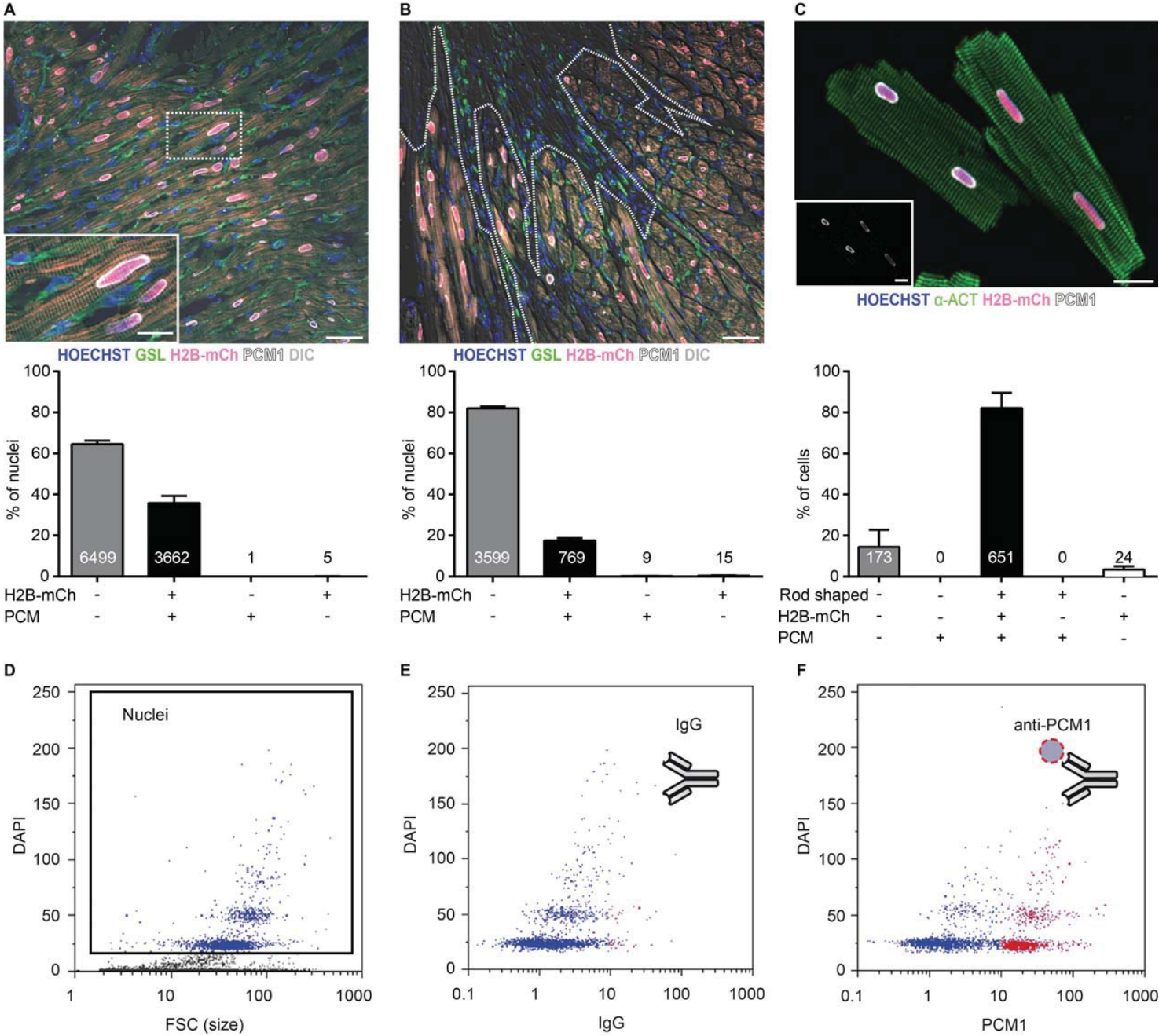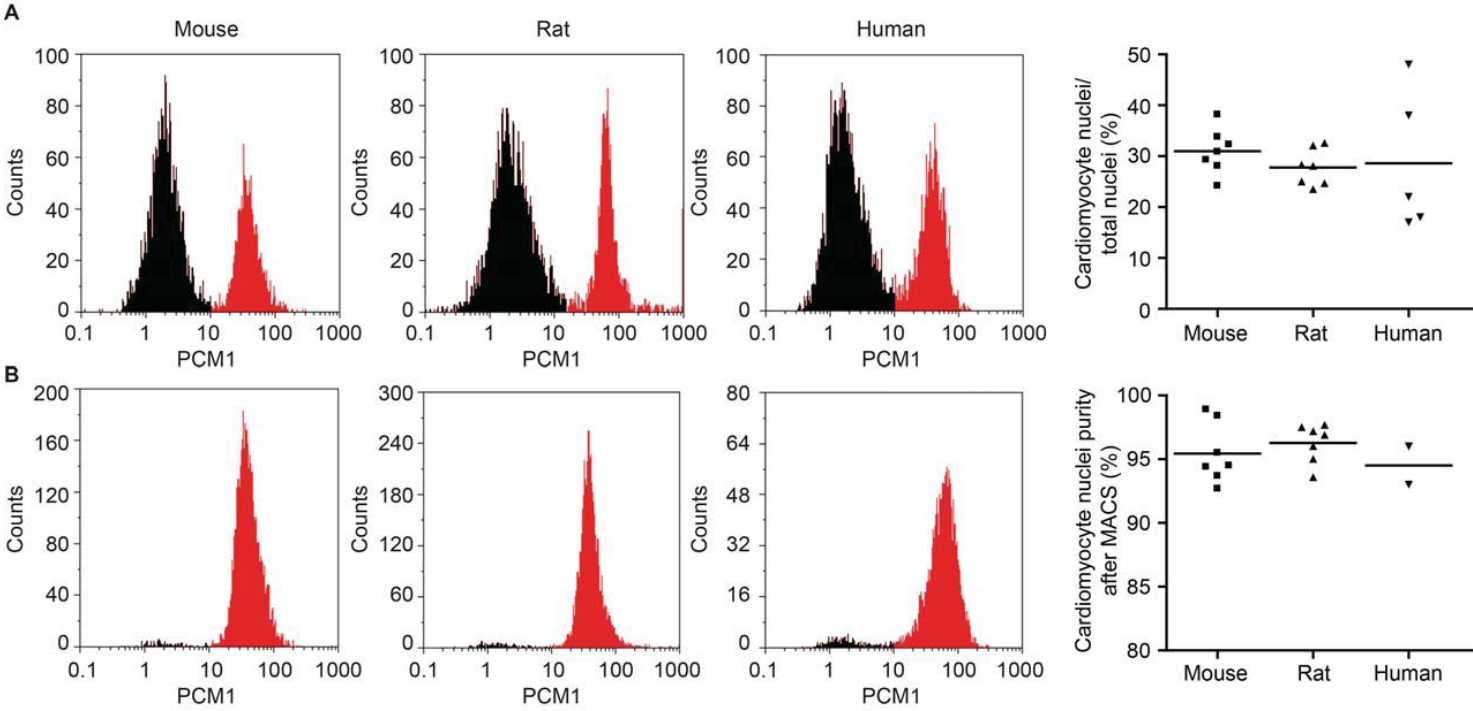MACS

Nuclear RNA-seq
ChIP-seq
MethylC-seq

B Isolation of cardiac cells

FACS

Cellular RNA-seq

FIGURE 2

FIGURE 3

FIGURE 4

A Pln

Transcript 1

Transcript 2

1 kb

Cellular RNA-seq

RPKM 2000 / 0

Nuclear RNA-seq

RPKM 3500 / 0

B

Unspliced mRNA (%)

***

Cellular mRNA / Nuclear mRNA

C

Uniquely mapped reads (%)

ncRNAs
mRNAs

Cellular mRNA / Nuclear mRNA

D

16 / 436

7,521 / 5,709

6,492

high (≥ 100 FPKM)
moderate (10 -100 FPKM)
low (1 - 10 FPKM)
very low (0.062 - 1 FPKM)
not detectable (≤ 0.062 FPKM)
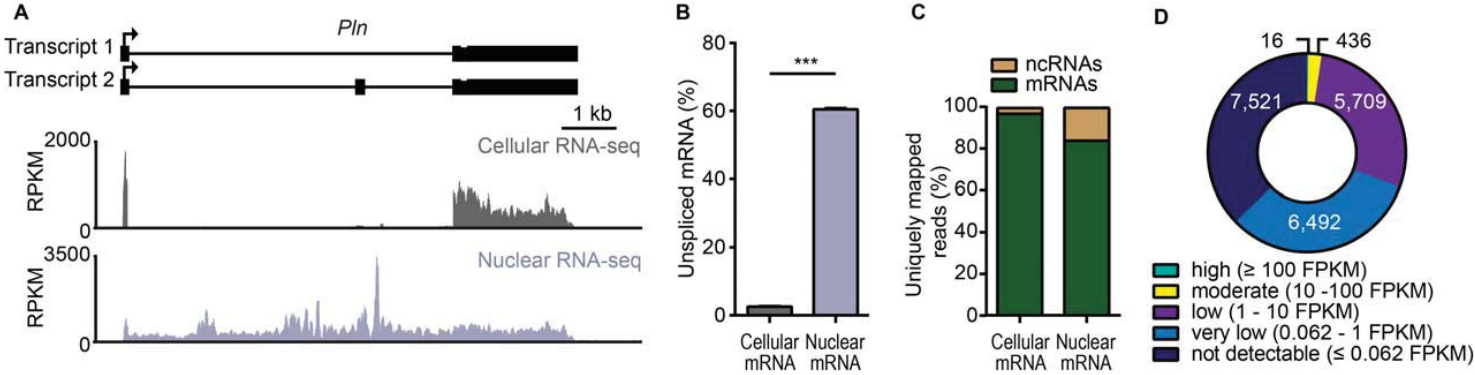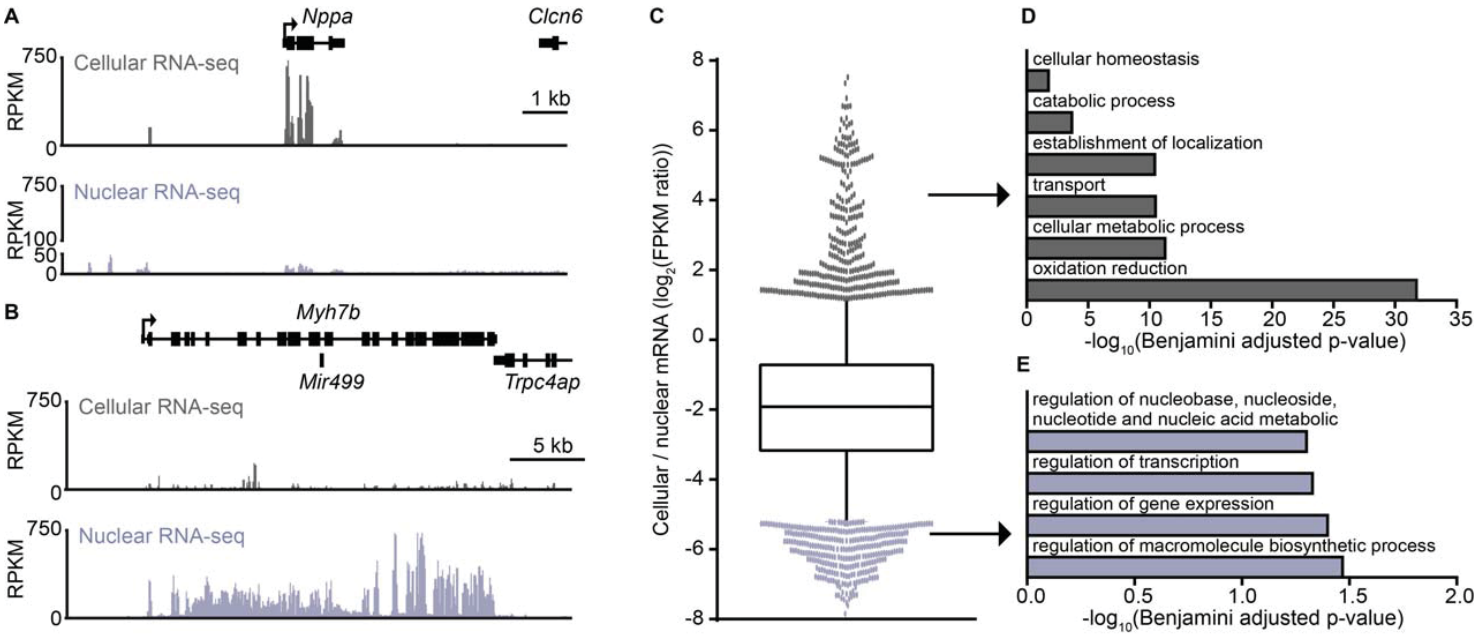
FIGURE 5

Cardiomyocyte nuclei

Hearts

FIGURE 6

A *Myl3*

C *Myl3*
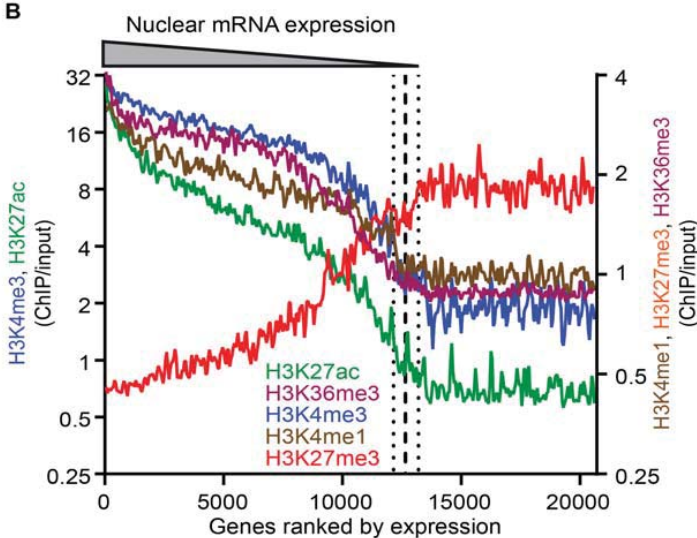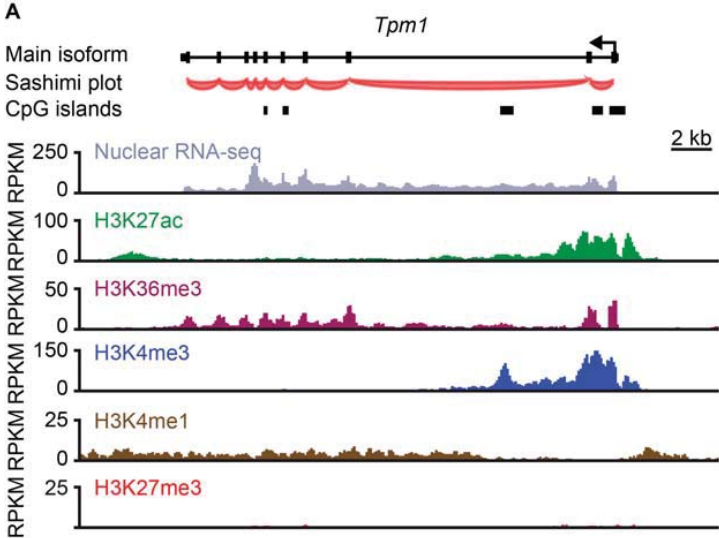
B *Vim*

D *Vim*
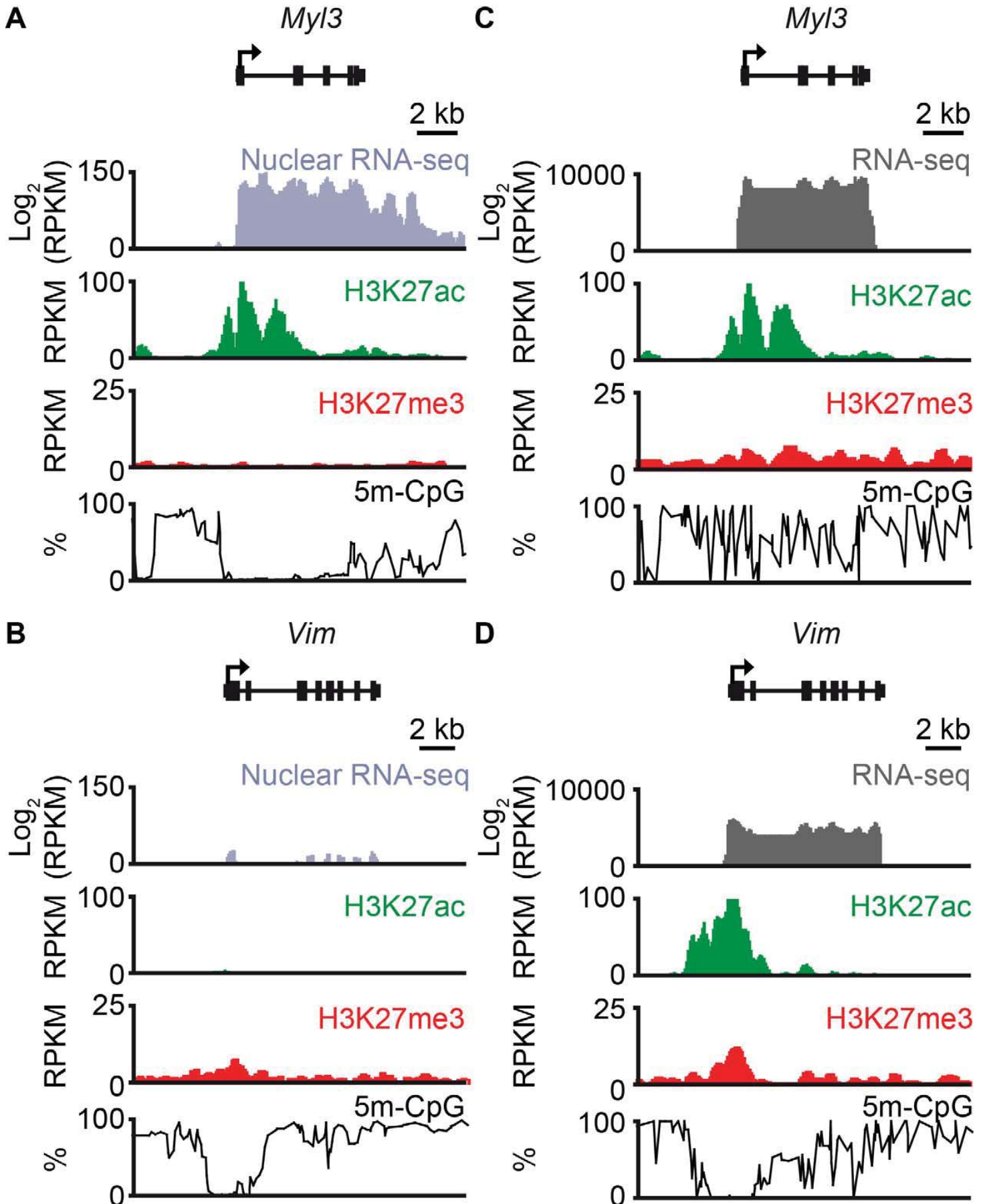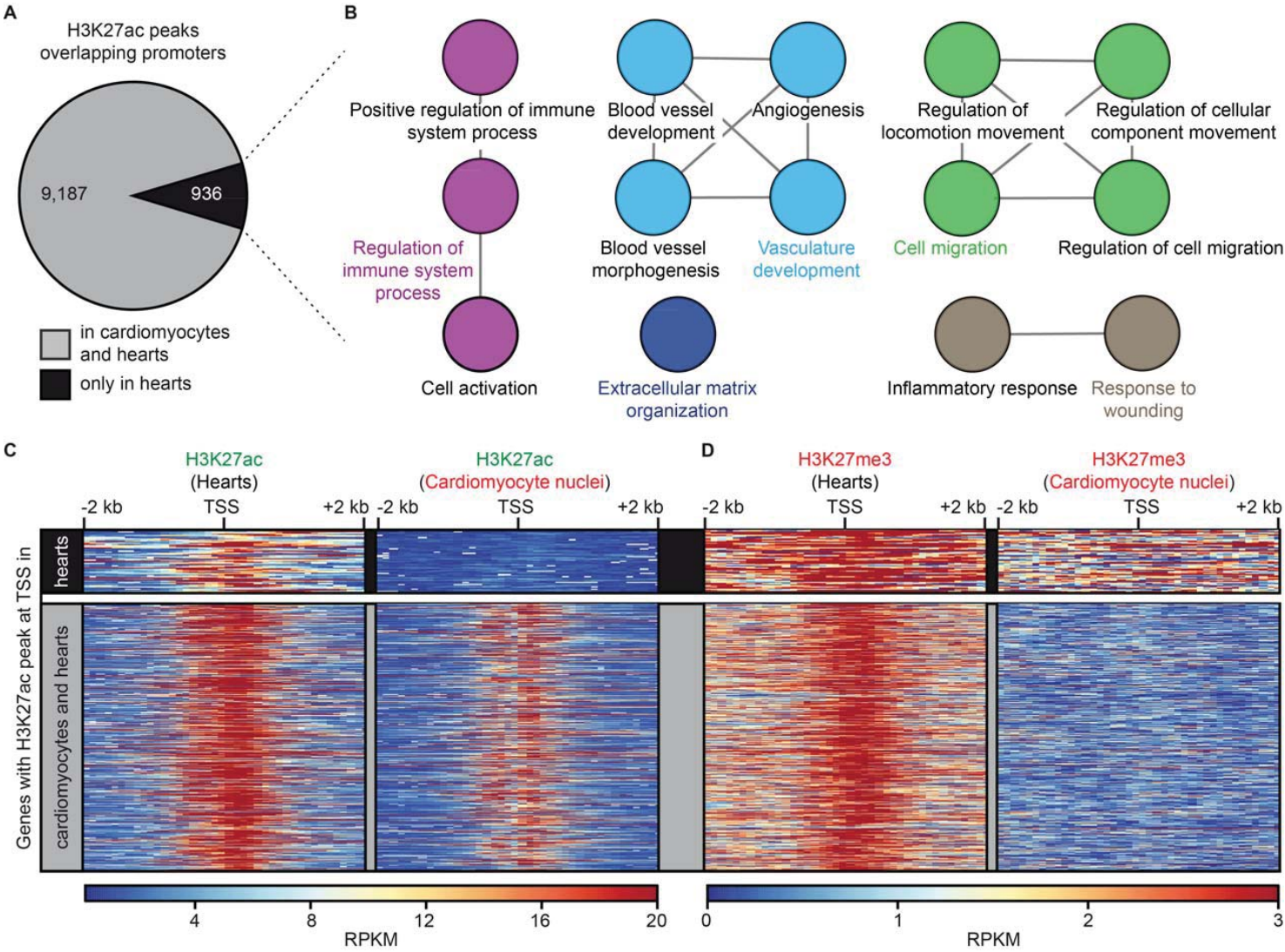
FIGURE 7

FIGURE 8
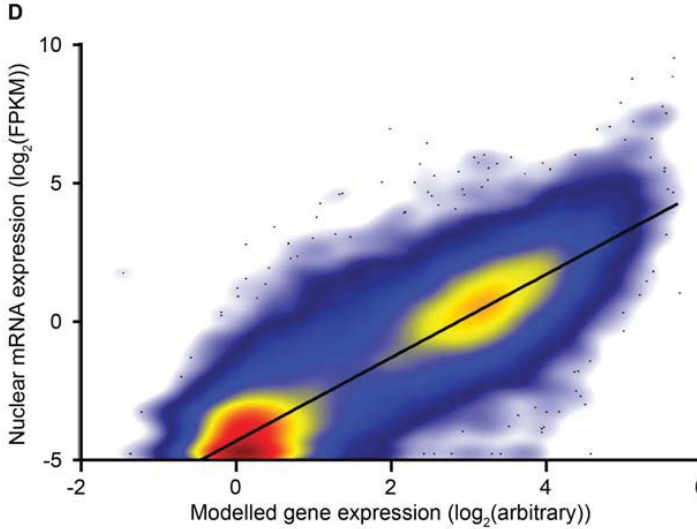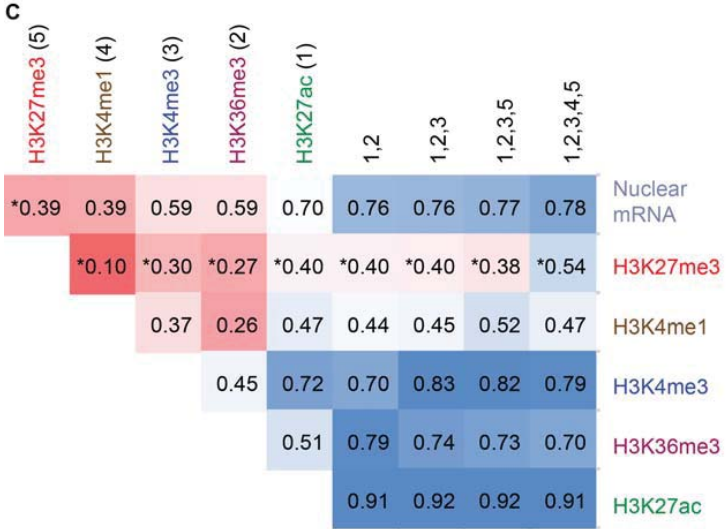
SUPPLEMENTAL MATERIAL

DETAILED METHODS

Animal procedures
All animal procedures were approved by the responsible animal care committee (Regierungspräsidium Freiburg, Germany) and the Landesamt für Natur, Umwelt und Verbraucherschutz, Recklinghausen, Germany); they conformed to the Guide for the Care and Use of Laboratory Animals published by the National Academy of Sciences 2011. Twelve weeks old male C57BL/6N mice, twelve weeks old female Myh6-H2B-mCherry transgenic mice[1] and Wistar rats were used. Experimental infarction by ligation of the left anterior descending coronary artery was performed as previously described[1]. Mice were sacrificed 10 days after infarction and hearts were perfusion fixed with 4% paraformaldehyde solution. After further fixation overnight, the hearts were treated with 20% sucrose solution and mounted in O.C.T compound.

Human cardiac biopsies
Left ventricular biopsies from non-failing hearts were used for cardiomyocyte nuclei isolation. These investigations were approved by the ethics committee of the University of Freiburg.

Immunohistochemistry
Frozen, formaldehyde fixed adult mouse hearts were sectioned into 10 µm slices with a cryotome CM 3050S (Leica).
Sections of mouse hearts were subjected to antigen retrieval (10 mM sodium citrate, pH 6.0, was performed in a KOS Microwave (Milestone, program: 4 min 70°C, 3 min 85°C, 4 min 90°C, 5 min 93°C). Cryo-sections were stained with antibodies against PCM1 (HPA023370, Sigma 1:1000 or G2000, Cell Signaling, 1:100). Isolated cardiomyocytes were stained with antibodies against α-actinin (1:400, clone EA-53, Sigma-Aldrich) and PCM-1 (G2000, Cell Signaling, 1:100). Primary antibodies were visualized by secondary antibodies conjugated to Cy2 and Cy5 (Life Technologies, 1:1000, Jackson ImmunoResearch 1:400). Griffonia simplicifolia lectin I (GSL-I, Vector Laboratories) or α-smooth muscle actin (ACTA2, A5228, Sigma 1:800) staining was used to visualize the glycocalyx of endothelial cells or α-smooth muscle cells, respectively. Nuclei were stained with DAPI (4',6-diamidino-2-phenylindole, Life technologies) and Hoechst 33342.
For documentation an inverted fluorescence microscope (Axiovert 200; Carl Zeiss MicroImaging, Inc.) equipped with a slider module (ApoTome2) and an inverted confocal laser scanning microscope (Eclipse Ti, Nikon) were used. Images were generated with ZEN 2012 software (Zeiss) and the NIS Elements software (Nikon).
For quantification of PCM1 positive or H2B-mCh positive nuclei in 10 µm thick tissue sections six 400 µm x 500 µm fields were analyzed per heart (n = 2). After experimental infarction at least eight fields (200 µm x 500 µm) within the border zone were analyzed for PCM1 positive or H2B-mCh positive nuclei (n = 2).
Ventricular cells from adult mice were enzymatically isolated with 1 mg/ml (activity 0.199 U/mg) Collagenase B and 33 µg/ml Trypsin by Langendorff perfusion as previously described[1]. Isolated cells were fixated with 4% formaldehyde solution. Isolated adult cardiomyocytes and non-cardiomyocytes were quantified after generation of maximum intensity projections of z-stacks. At least 130 ventricular cardiomyocytes per heart (n = 4) were checked for the overlap of H2B-mCh expression and PCM1 staining.

Isolation of cardiac nuclei
Cardiac nuclei were isolated as previously described[2]. All steps of the protocol were carried out at ≤ 4 °C. Protease-inhibitors (cOmplete Protease Inhibitor Cocktail, Roche) and DDT (1 mM, dithiothreitol) were freshly prepared and added to all buffers. For the isolation of nuclear RNA, RNAsin (80 U/ml, Promega) was added to all buffers. For chromatin isolation sodium butyrate (10 mM) was added. Snap frozen cardiac tissue was thawed on ice and 3 ml lysis buffer (5 mM $CaCl_2$, 3 mM MgAc, 2 mM EDTA, 0.5 mM EGTA, 10 mM Tris-HCL,

pH 8) was added. The tissue was homogenized using a gentleMACS dissociator (Miltenyi) with gentleMACS M tubes (Miltenyi) using the protocol "protein_01". Next, 3 ml of lysis buffer supplemented with 0.4 % triton-X was added and the combined cell suspension was filtered through 40 µm gaze (BD Biosciences). The filter was washed with 2 ml lysis buffer including 0.2 % triton-X. The flow-through was centrifuged (1000 x g, 5min). The pellet was resuspended and overlayed on 1 M sucrose (3 mM MgAc, 10 mM Tris-HCl, pH 8). After centrifugation (1000 x g, 5 min) the pellet was resuspended in 500 µl staining buffer (PBS containing 5 % BSA and 0.2 % Igepal CA-630) and used for magnetic-assisted purification or FACS.

Magnetic-assisted sorting of cardiomyocyte nuclei
All steps of the protocol were carried out at ≤ 4°C. For magnetic-assisted sorting, cardiomyocyte nuclei were incubated with an anti-PCM1 antibody (1:1,000, Sigma) in staining buffer. After staining nuclei were centrifuged. Nuclei were resuspended with 20 µl anti-rabbit IgG MicroBeads (Miltenyi) and 80 µl MACS buffer (PBS containing 2 mM EDTA, 1 % BSA, 2 % skimmed milk powder) and incubated for 15°C. After addition of 900 µl MACS buffer the suspension was applied to MS columns (Miltenyi), washed with 3 ml MACS buffer and eluted. This step was repeated once using another MS column (Miltenyi). Cardiomyocyte nuclei were finally eluted in PBS containing 1 mM EDTA. Sorting purity was validated by flow cytometric analysis after staining with an Alexa647-labelled secondary anti-rabbit antibody (1:1,000, Life Technologies) and DAPI (1:1,000, Life Technologies) using a CyFlow Space (Partec).

Flow cytometric analysis and sorting of cardiac myocyte nuclei
Cardiomyocyte nuclei were incubated with an anti-PCM1 antibody (1:1000, HPA023370, Sigma) or isotype control IgG (1:10000, ab37415, Abcam) and Alexa-labeled secondary anti-rabbit antibodies (1:1000, Life technologies). For nuclei staining DAPI (1:1000, Life technologies) or Draq7 (1:200, Life technologies) were used. Nuclei were analyzed (CyFlow Space, Partec) or sorted (Bio-Rad S3, Bio-Rad) by flow cytometry.

Isolation of cardiac cells and sorting of viable cardiomyocytes
Adult mouse hearts were digested to obtain a single-cell suspension by retrograde perfusion[3, 4] with 15 ml Tyrode's solution supplemented with 25 mM butanedione monoxime, 2 mM CaCl$_2$, 0.8 mg ml^{-1} collagenase B (Roche, Mannheim, Germany), 0.4 mg ml^{-1} hyaluronidase (Sigma) and 3 µg ml^{-1} trypsin (Sigma) for 12 min. The enzymatic digestion was stopped by addition of 20 ml buffer S (Tyrode's buffer, 5% FCS, 25 mM butanedione monoxime, 2 mM CaCl$_2$). Hearts were gently dissected into small pieces using a pair of forceps following repetitive pipetting (10-20x) using a serological pipette. The resulting suspension was filtered through 100 µm gaze (Greiner Bio-One) and centrifuged with low force (50 x g, 5 min, 4 °C). The pellet was resuspended in 4 ml buffer S (4 °C). Flow cytometric analysis and sorting of cardiomyocytes was carried out at 4 °C using a Bio-Rad S3 cell sorter. Cardiomyocytes and non-cardiomyocytes were visualized using the cell-permeable nucleic acid stain DRAQ5 (Cell Signaling Technology). Sorting of viable cardiomyocytes was performed after addition of the cell-impermeable nucleic acid dye DRAQ7 (Life Technologies). Cardiomyocytes were discriminated from other cardiac cells by high forward scatter (FSC) signals. Gates were selected to sort viable cardiomyocytes directly into RLT lysis buffer (Qiagen, Hilden, Germany).

ChIP-sequencing
ChIP-seq was performed as described previously with modifications[2, 5]. Purified cardiomyocyte nuclei were fixed with 1 % PFA (paraformaldehyde, Sigma) for 2 min at room temperature. Fixation was quenched by adding glycine to a final concentration of 125 mM. After washing with PBS for three times, nuclei were lysed in SDS buffer (50 mM Tris-HCl pH 8.0, 10 mM EDTA, 1 % SDS) supplemented with protease inhibitors (cOmplete Protease Inhibitor Cocktail, Roche). Chromatin was sonicated using a Bioruptor® (Diagenode) with 30 cycles (30 s on/30 s off; high energy) to an average fragment size of 200 – 400 bp. 200 µl

Protein A Dynabeads (Life technologies) were washed with TE buffer (20 mM Tris-HCl pH 8.0, 2 mM EDTA) two times. Following the second wash step, beads were resuspended in 1 ml TE buffer containing 1 mg/ml tRNA (Sigma) and 1 mg/ml BSA (Roth). After incubation for 2 h at 4 °C, beads were washed with TE buffer three times and finally resuspended in 200 µl TE. Chromatin concentration was adjusted to 50 ng/µl using SDS buffer. Next, chromatin was diluted 1:10 with dilution buffer (50 mM HEPES-KOH pH 7.5, 500 mM NaCl, 1 mM EDTA, 1 % Triton X-100, 0.1 % sodium deoxycholate, 0.1 % SDS, protease inhibitors) and precleared with 10 µl blocked beads for 1 h at 4 °C. 50 µl of pre-blocked chromatin served as input. For immunoprecipitation 2.5 µg of chromatin was incubated with an anti-H3K36me3 antibody (1 µg, ab9050, Abcam) overnight. The next day, 15 µl blocked beads were added and samples were incubated for 3 h at 4 °C. Immunocomplexes were washed for 5 min each with dilution buffer for two times, with wash buffer (10 mM Tris-HCl pH 8.0, 250 mM LiCl, 1 mM EDTA, 0.5 % IGEPAL CA-630, 0.5 % sodium deoxycholate) and finally with TE buffer (20 mM Tris-HCl pH 8.0, 2 mM EDTA) at 4 °C. Following magnetic separation, beads were resuspended in 160 µl elution buffer (100 mM $NaHCO_3$, 1 % SDS) and immunocomplexes were eluted by incubation at room temperature for 15 min. This step was repeated with another 160 µl of elution buffer. The eluates were combined and treated with 20 ng/µl RNAse A (Sigma) for 30 min at 37 °C. Crosslinks were reversed by adding 0.5 µg/µl proteinase K (AppliChem) and incubation at 55 °C for 2.5 h. After this initial incubation, temperature was raised to 65 °C and incubated overnight. DNA was purified using phenol/chloroform followed by ethanol precipitation at -20 °C overnight. DNA was quantified using Quant-iT™ PicoGreen® dsDNA Reagent (Life technologies) and 5 ng were used per library. NEBNext® ChIP-seq Library Prep Master Mix Set for Illumina (NEB) was used for library preparation (15 PCR cycles). Libraries were sequenced on a HiSeq™ 2500 (50 bp, paired-end, Illumina). Data were deposited to the NCBI BioSample database (SRP033385).

Gene expression analysis
Total RNA was isolated from intact cardiomyocytes as previously described[2] or from cardiomyocyte nuclei from one adult mouse heart using RNeasy Micro Kit (Qiagen) including on-column DNAse digestion. Ribosomal RNA was depleted using the Low Input RiboMinus Eukaryote System v2 (Life technologies). Depleted RNA fragmented to approximately 200 bp fragments and was used for library construction (NEBNext® Ultra RNA Library Prep Kit for Illumina, NEB). Size selection was performed with AMPure® XP Beads (Beckman Coulter) according to the NEBNext® Ultra RNA Library Prep Kit manual. 15 PCR cycles were used for amplification. Libraries were sequenced on a HiSeq 2500 (50 bp, paired-end, Illumina). Data were deposited to the NCBI BioSample database (SRP033386).

Bioinformatics analysis
All bioinformatics tools used in this study were used as part of the Galaxy platform[6]. The *Mus musculus* genome (mm9) and the annotation of protein coding genes and CpG islands provided by the UCSC was used as a basis for data analysis[7]. RNA class assignment of non-protein coding genes was obtained from the Ensembl mm9 annotation[8].

RNA sequencing reads were mapped using Tophat2[9] and duplicate reads were removed. Cufflinks[10] was used to estimate transcript abundance as fragments per kilobase of exon per million mapped reads (FPKM). The spliced fraction of cardiomyocyte nuclear RNA was used to determine the main cardiomyocyte isoform of each gene. This isoform was used for all subsequent analysis steps. To estimate the detection limit of nuclear RNA-seq, 2 Mb of randomly selected genomic regions outside of genes and flanking regions (± 5 kb) were added to the analysis. The resulting mean FPKM was regarded as detection limit.

ChIP-seq reads were mapped using Bowtie2[11]. To identify genomic regions enriched for H3K27ac MACS2[12] was used. A detection q-value of 0.01 was regarded as significant. GREAT[13] was used to identify peak associated genes and to perform subsequent gene ontology analysis. DeepTools[14] were used for data visualization and normalization.

Prediction of gene expression
The analysis was limited to the main cardiomyocyte gene isoforms. Transcripts with expression values below the detection limit overlapping expressed genes were removed from further analysis steps, leaving 17,915 coding genes for fur further analysis.

To obtain the sum of tag counts we counted reads for each modification using HTSeq-count[15]. For H3K4me3 and H3K27ac reads overlapping the TSS (± 2 kb) were selected to determine reads per kilobase per million mapped reads (RPKM). For H3K36me3, H3K4me1 and H3K27me3 the gene body was used to calculate RPKM values. We normalized the resulting sum of tags to the respective values of whole cell extract chromatin (WCE).

Results from RNA-seq and ChIP-seq experiments were subjected to additive smoothing using an α value. The α value was chosen which maximized the correlation by an iteration over a search space from 0 to 1.

Linear regressions of log-transformed values were used to model the relationship of different histone marks and transcript levels followed by calculation of the pearson coefficient (r^2). The sum of log-transformed values of different histones were calculated to increase the goodness of fit. Histone modifications were added subsequently to the combinatorial model according to their coefficient of variation.

External data sets
Previously published MethylC-seq data and ChIP-seq data (H3K27ac, H3K4me3, H3K4me1 and H3K27me3) from adult cardiomyocyte nuclei were analyzed as described[2]. ChIP-seq data for H3K27me3[16] and H3K27ac[17], methylC-seq data[18] and RNA-seq data[17] derived from adult hearts were reanalyzed. H3K27me3, H3K27ac and H3K4me3 data from *in vitro* differentiated cardiomyocytes[19] were reanalyzed. RNA-seq data from 8 week old mice of non-cardiac tissues were reanalyzed[20], too.

Gene ontology analysis
Enriched GO terms of the category 'biological process' were identified by ClueGO[21]. The resulting p-values were corrected for multiple testing using the Benjamini-Hochberg equation. The most significant term of each group was highlighted.
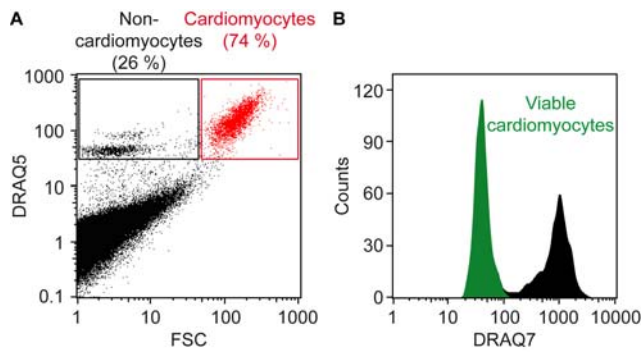
Online Figure I: Flow cytometric analysis of cardiomyocytes after Langendorff perfusion.
A FACS analysis of a cell suspension after Langendorff perfusion of a wild-type mouse heart. Cells were identified by staining with the membrane-permeable fluorescent dye DRAQ5. The representative dot plot illustrates identification of cardiomyocytes according to high FSC values (red box) as compared to non-cardiomyocytes (black box). The portion of non-cardiomyocytes after Langendorff perfusion was 19 ± 4 % (n = 4, mean ± SEM). **B** Viability of cardiomyocytes was assessed by the membrane-impermeable dye DRAQ7. Viable cardiomyocytes showed low fluorescence (green population) and were sorted.
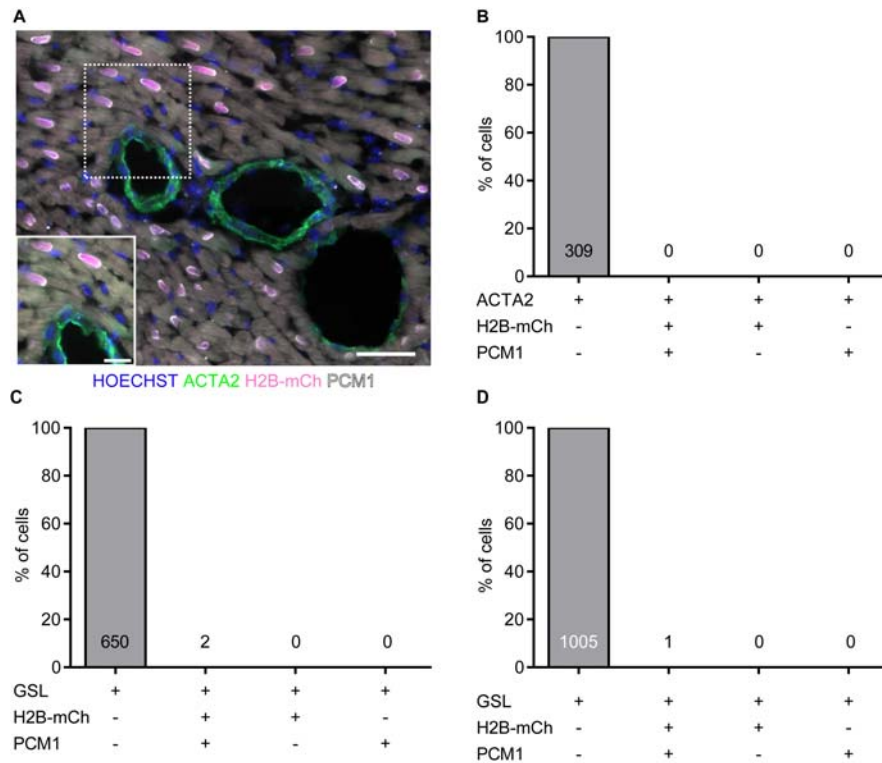
Online Figure II: PCM1 staining of cardiac endothelial and smooth muscle cells.
A Cryosections of adult Myh6-H2B-mCh transgenic hearts were stained with PCM1. Nuclei were stained with Hoechst 33342 and smooth muscle cells were identified by α-smooth muscle actin (ACTA2, scale bars: 50 µm in overviews, 20 µm in close-up). **B** Quantification of PCM1 staining and H2B-mCh expression in ACTA2 positive cells (n = 2 hearts, numbers indicate total counted cells). **C, D** Quantification of PCM1 staining and H2B-mCh expression in GSL stained endothelial cells of adult Myh6-H2B-mCh transgenic mouse hearts. Analysis of cryosections (see Figure 2A, B) of native hearts (**C**) and the border zone of infarcted hearts 10 days after left coronary ligation (**D**) (n = 2 native and n = 2 infarcted hearts, numbers indicate total counted cells).
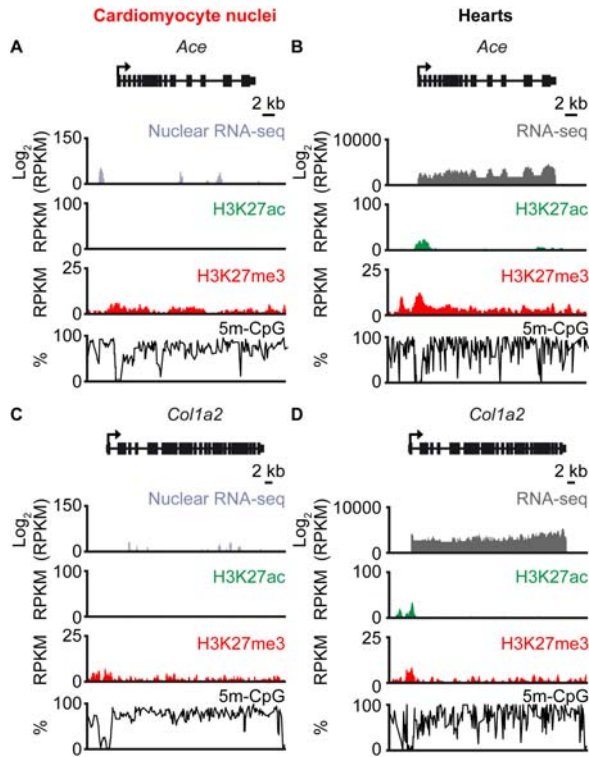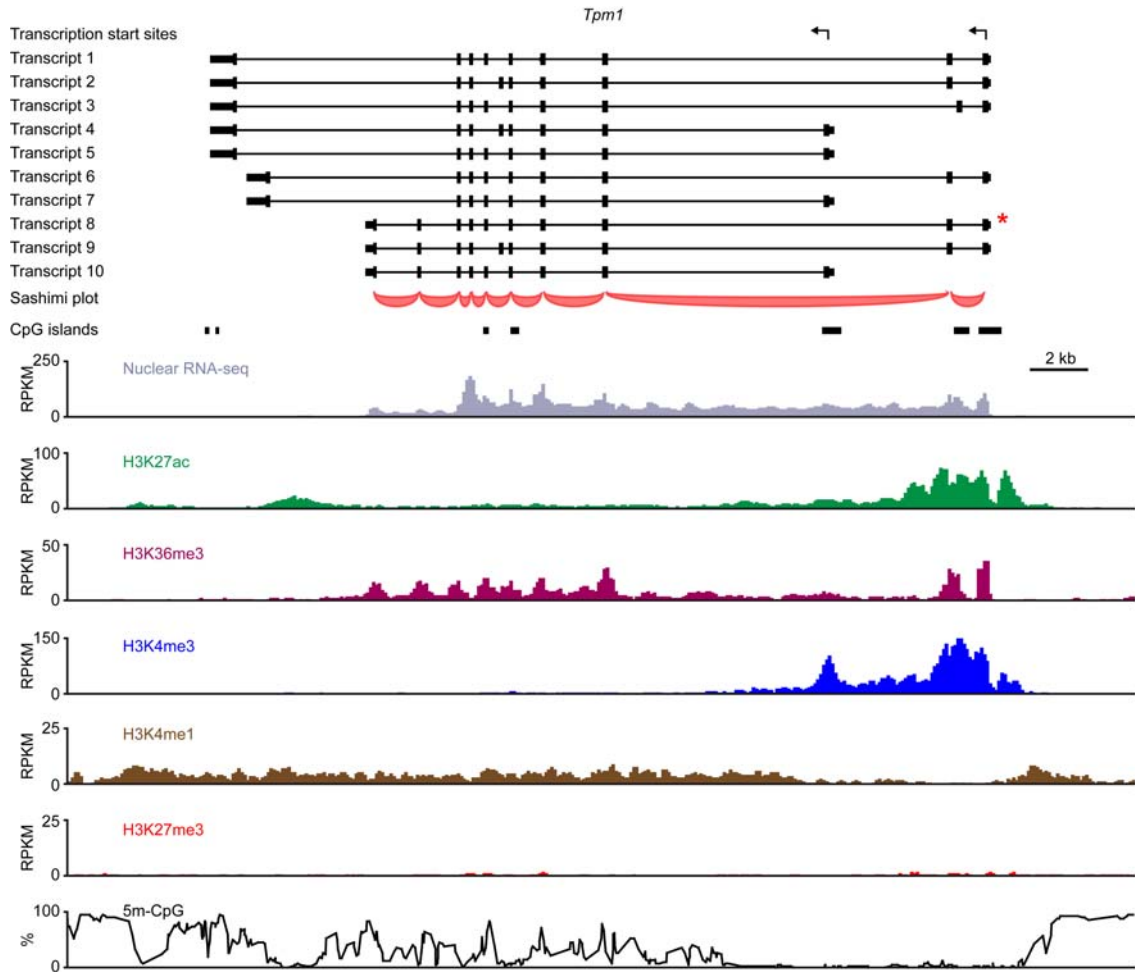
Online Figure III: Epigenetic signature of representative non-cardiomyocyte genes.
Exemplary IGV traces illustrating mRNA expression, histone marks and DNA methylation
(5m-CpG) maps for the endothelial cell gene angiotensin converting enzyme (*Ace*, A, B) and
the fibroblast gene collagen alpha-2(I) chain (*Col1a2*, C, D; RPKM: reads per kilobase of
exon per million mappable reads).
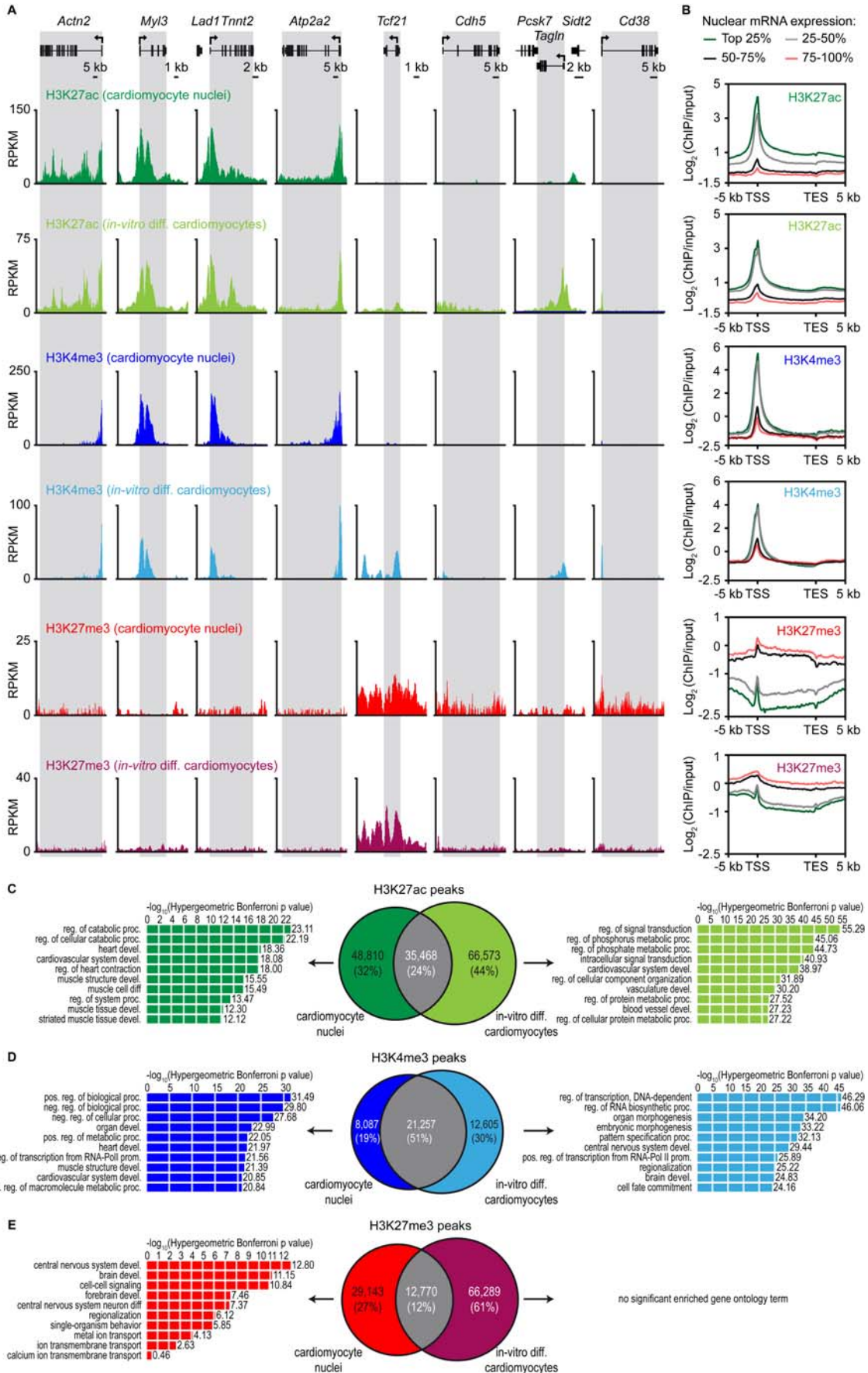
Online Figure IV: Comparison of ChiP-seq data from *in-vitro* differentiated cardiomyocytes and cardiomyocyte nuclei.

A Exemplary IGV traces illustrating read density of active histone marks H3K4me3 and H3K27ac and the polycomb mark H3K27me3 are shown for cardiomyocyte nuclei and *in vitro* differentiated cardiomyocytes[19]. Results are shown for the cardiomyocyte genes alpha-actinin 2 (*Actn2*), myosin light chain 3 (Myl3), cardiac troponin T type 2 (*Tnnt2*) and sarcoplasmic reticulum calcium ATPase 2 (*Atp2a2*). In addition, profiles of the fibroblast-specific transcription factor gene (*Tcf21*)[22], the endothelial cell gene VE-cadherin (*Cdh5*)[23], the smooth muscle cell gene transgelin (*Tagln*)[24] and the leukocyte marker gene cluster of differentiation 38 (*Cd38*)[25] are depicted. Patterns for cardiomyocyte genes were almost identical. Non-cardiomyocyte genes were marked by active histone marks exclusively in *in vitro* differentiated cardiomyocytes indicating presence of cell types expressing *Tcf21*, *Cdh5*, *Tagln*, or *Cd38*. Cardiomyocyte genes and *Tagln* were depleted for H3K27me3 in both data sets. The remaining non-cardiomyocyte genes were enriched for H3K27me3 in cardiomyocyte nuclei but not in *in vitro* differentiated cardiomyocytes (RPKM: reads per kilobase of exon per million mappable reads). **B** Summary plots for H3K4me3, H3K27ac and H3K27me3 in cardiomyocyte nuclei and *in-vitro* differentiated cardiomyocytes[19]. Genes were grouped in quartiles according to expression values in cardiomyocyte nuclei. This genome-wide analysis revealed similar enrichment profiles for the indicated histone marks in cardiomyocyte nuclei and *in vitro* differentiated cardiomyocytes (TSS: transcription start site; TES: transcription end site). **C-E** Venn diagrams illustrating the overlap of H3K27ac **(C)**, H3K4me3 **(D)** and H3K27me3 **(E)** peaks detected in *in vitro* differentiated cardiomyocytes[19] and cardiomyocyte nuclei. Numbers and percentages indicate the absolute and relative number of peaks. Gene ontology analysis was performed with the nearest peak associated gene (100 kb window). Bar graphs show enriched terms specific for either *in vitro* differentiated cardiomyocytes (right part) or cardiomyocyte nuclei (left part) determined for H3k27ac **(C)**, H3K4me3 **(D)** and H3K27me3 **(E)**. Shown are the ten most significant terms. Values at bar ends indicate Bonferroni corrected negative base 10 logarithms of hypergeometric p values.

**Online Figure V: Isoform identification and epigenetic signature of *Tpm1*.**
Depicted are the annotated Refseq gene isoforms of tropomyosin 1 (*Tpm1*). Reads spanning exon-exon junctions are marked by arcs (Sashimi plot). The main isoform identified by RNA-seq is highlighted (red asterisk). Histone profiles and DNA methylation signatures supported RNA-seq splicing analysis (RPKM: reads per kilobase per million mapped reads).
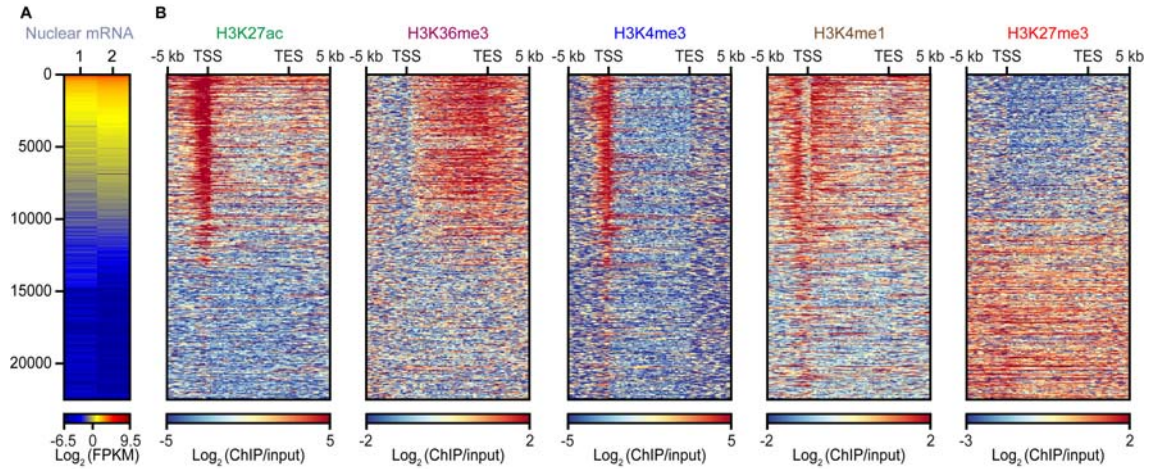
Online Figure VI: Heat maps of nucRNA and histone profiles in cardiomyocyte nuclei
A Expression values of nucRNA in cardiomyocytes as measured by RNA-seq for two independent biological replicates. Genes were ranked according to mean expression levels.
B Corresponding histone modification profiles of gene bodies and flanking regions. Shown are results for the main isoform of coding genes annotated by the UCSC[7] (TSS: transcription start site; TES: transcription end site).
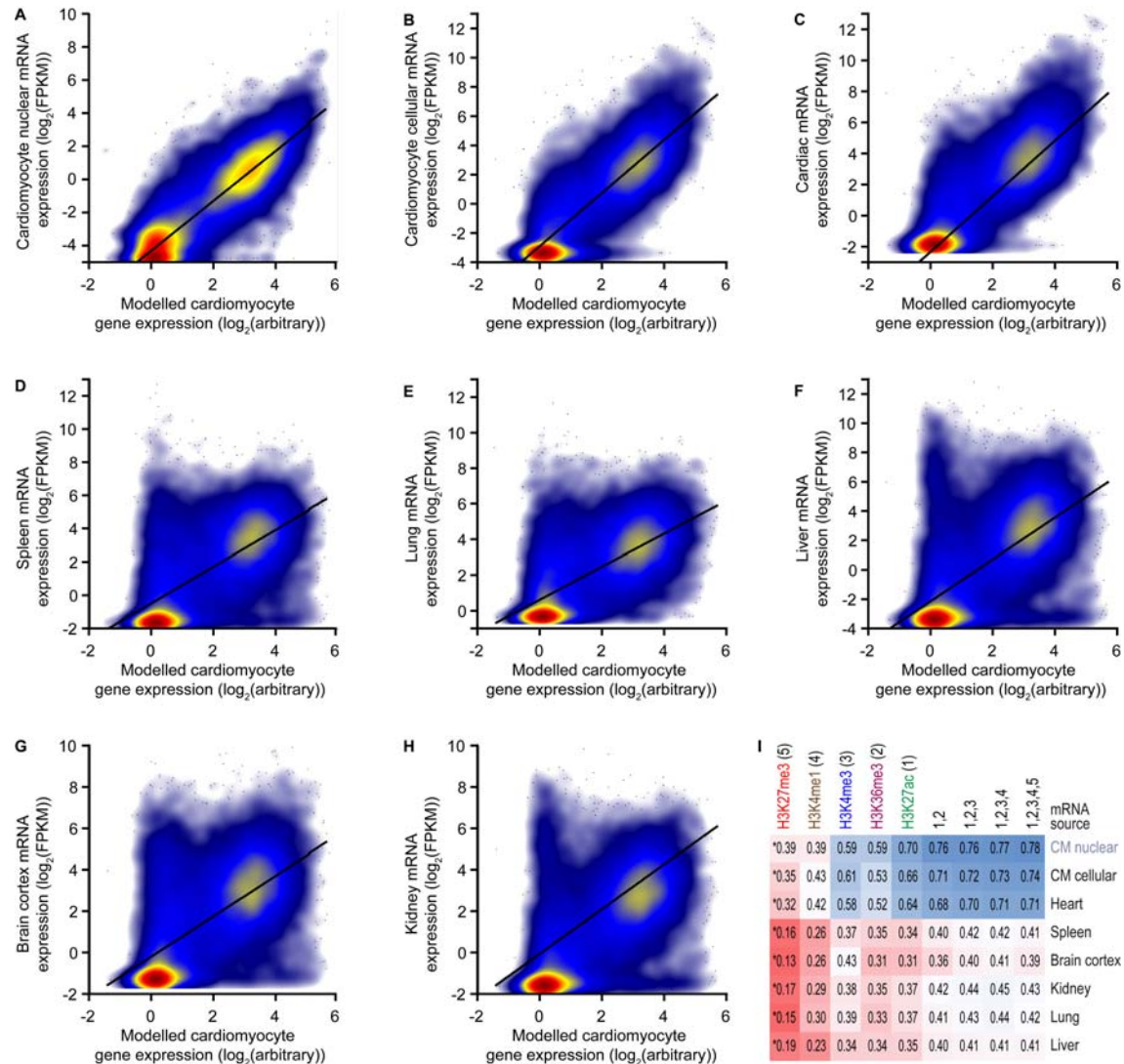
Online Figure VII: Relationship between histone modifications in cardiomyocytes and gene expression in cardiomyocytes, hearts and non-cardiac tissues.
A-H Scatterplots with RNA expression values predicted form the full set of histones on the x axes. On the y axes are measured RNA expression values in cardiomyocyte nuclei (**A**), cardiomyocytes (**B**), hearts (**C**), spleen (**D**), lung (**E**), liver (**F**), brain cortex (**G**) and kidney (**H**). The black lines represent the linear fit in between modeled and measured expression. Colors represent the density of points. Regions were marked by darkblue, light blue, yellow, red and darkred in order of increasing densities. **I** Determination coefficient (r^2) heatmaps of different histone mark enrichments in cardiomyocytes, linear models including different combinations of these histone marks and RNA expressions values in cardiomyocytes (CM, nuclear and cellular), hearts and non-cardiac tissues of adult mice (* indicates inverse correlation).

Application	Substrate	Sorting method	Mass (µg)	Nuclei/ cells (no., x 10^5)	Hearts (no.)
MethylC-seq	DNA	FACS/ MACS	1.2	6	3
ChIP-seq	Chromatin	MACS	2.5	2	1
nuclear RNA-seq	RNA	FACS	n.d.	2	1
cellular RNA-seq	RNA	FACS	n.d.	≥0.01	1

Online Table I: Experimental details
The table illustrates the amounts of adult mouse hearts to derive the indicated numbers of nuclei or cells by the suggested sorting method. The listed numbers were compatible with the provided methods to study epigenetic modifications or gene expression.

RNA class	cellular RNA-seq (%)	nuclear RNA-seq (%)
linc	1.14	8.15
antisense	0.33	0.75
misc	0.25	0.22
non-coding	0.08	1.89
processed transcript	0.08	0.49
pseudogene	0.80	2.66
sense intronic	0.00	0.02
miRNA	0.47	0.30
snRNA	0.00	0.03
snoRNA	0.03	0.17
protein coding	96.81	85.30

Online Table II: Analysis of different RNA classes
The table illustrates the fraction of RNA-seq fragments mapping to specific RNA classes listed in the Ensembl mm9 annotation. Shown are results of RNA classes with at least 0.01% of RNA-seq reads in either cellular or nuclear RNA-seq of cardiomyocytes. (Abbreviations: linc, long intergenic non-coding RNA; antisense, RNA transcribed from the opposite strand of a mRNA locus; misc, miscellaneous other RNA; non-coding, non-coding RNA; processed transcript, transcript lacking an open reading frame; sense intronic, non-coding transcript overlapping only intronic regions; miRNA, microRNA precursors; snRNA, small nuclear RNA; snoRNA, small nucleolar RNA; protein coding, protein coding mRNA)

REFERENCES

1. Raulf A, Horder H, Tarnawski L, Geisen C, Ottersbach A, Roll W, Jovinge S, Fleischmann BK and Hesse M. Transgenic systems for unequivocal identification of cardiac myocyte nuclei and analysis of cardiomyocyte cell cycle status. *Basic Res Cardiol.* 2015;110:489.
2. Gilsbach R, Preissl S, Gruning BA, Schnick T, Burger L, Benes V, Wurch A, Bonisch U, Gunther S, Backofen R, Fleischmann BK, Schubeler D and Hein L. Dynamic DNA methylation orchestrates cardiomyocyte development, maturation and disease. *Nat Commun.* 2014;5:5288.
3. Bell RM, Mocanu MM and Yellon DM. Retrograde heart perfusion: the Langendorff technique of isolated heart perfusion. *J Mol Cell Cardiol.* 2011;50:940-50.
4. Roth GM, Bader DM and Pfaltzgraff ER. Isolation and physiological analysis of mouse cardiomyocytes. *J Vis Exp.* 2014:e51109.
5. Tippmann SC, Ivanek R, Gaidatzis D, Scholer A, Hoerner L, van Nimwegen E, Stadler PF, Stadler MB and Schubeler D. Chromatin measurements reveal contributions of synthesis and decay to steady-state mRNA levels. *Mol Syst Biol.* 2012;8:593.
6. Blankenberg D, Von Kuster G, Coraor N, Ananda G, Lazarus R, Mangan M, Nekrutenko A and Taylor J. Galaxy: a web-based genome analysis tool for experimentalists. *Curr Protoc Mol Biol.* 2010;Chapter 19:Unit 19 10 1-21.
7. Rosenbloom KR, Armstrong J, Barber GP, et al. The UCSC Genome Browser database: 2015 update. *Nucleic Acids Res.* 2015;43:D670-81.
8. Cunningham F, Amode MR, Barrell D, et al. Ensembl 2015. *Nucleic Acids Res.* 2015;43:D662-9.
9. Kim D, Pertea G, Trapnell C, Pimentel H, Kelley R and Salzberg SL. TopHat2: accurate alignment of transcriptomes in the presence of insertions, deletions and gene fusions. *Genome Biol.* 2013;14:R36.
10. Trapnell C, Williams BA, Pertea G, Mortazavi A, Kwan G, van Baren MJ, Salzberg SL, Wold BJ and Pachter L. Transcript assembly and quantification by RNA-Seq reveals unannotated transcripts and isoform switching during cell differentiation. *Nat Biotechnol.* 2010;28:511-5.
11. Langmead B, Trapnell C, Pop M and Salzberg SL. Ultrafast and memory-efficient alignment of short DNA sequences to the human genome. *Genome Biol.* 2009;10:R25.
12. Zhang Y, Liu T, Meyer CA, Eeckhoute J, Johnson DS, Bernstein BE, Nusbaum C, Myers RM, Brown M, Li W and Liu XS. Model-based analysis of ChIP-Seq (MACS). *Genome Biol.* 2008;9:R137.
13. McLean CY, Bristor D, Hiller M, Clarke SL, Schaar BT, Lowe CB, Wenger AM and Bejerano G. GREAT improves functional interpretation of cis-regulatory regions. *Nat Biotechnol.* 2010;28:495-501.
14. Ramirez F, Dundar F, Diehl S, Gruning BA and Manke T. deepTools: a flexible platform for exploring deep-sequencing data. *Nucleic Acids Res.* 2014;42:W187-91.
15. Anders S, Pyl PT and Huber W. HTSeq-a Python framework to work with high-throughput sequencing data. *Bioinformatics.* 2015;31:166-9.
16. Consortium EP. An integrated encyclopedia of DNA elements in the human genome. *Nature.* 2012;489:57-74. Data set SRX185852 (Bing Ren lab, Ludwig Institue for Cancer Research).
17. Shen Y, Yue F, McCleary DF, Ye Z, Edsall L, Kuan S, Wagner U, Dixon J, Lee L, Lobanenkov VV and Ren B. A map of the cis-regulatory sequences in the mouse genome. *Nature.* 2012;488:116-20.
18. Hon GC, Rajagopal N, Shen Y, McCleary DF, Yue F, Dang MD and Ren B. Epigenetic memory at embryonic enhancers identified in DNA methylation maps from adult mouse tissues. *Nat Genet.* 2013;45:1198-206.

19.	Wamstad JA, Alexander JM, Truty RM, et al. Dynamic and coordinated epigenetic regulation of developmental transitions in the cardiac lineage. *Cell.* 2012;151:206-20.
20.	Consortium EP. An integrated encyclopedia of DNA elements in the human genome. *Nature.* 2012;489:57-74. Data sets from study SRP012040 (Thomas Gingeras lab - Cold Spring Harbor Laboratory).
21.	Bindea G, Mlecnik B, Hackl H, Charoentong P, Tosolini M, Kirilovsky A, Fridman WH, Pages F, Trajanoski Z and Galon J. ClueGO: a Cytoscape plug-in to decipher functionally grouped gene ontology and pathway annotation networks. *Bioinformatics.* 2009;25:1091-3.
22.	Acharya A, Baek ST, Huang G, Eskiocak B, Goetsch S, Sung CY, Banfi S, Sauer MF, Olsen GS, Duffield JS, Olson EN and Tallquist MD. The bHLH transcription factor Tcf21 is required for lineage-specific EMT of cardiac fibroblast progenitors. *Development.* 2012;139:2139-49.
23.	Wang Y, Nakayama M, Pitulescu ME, et al. Ephrin-B2 controls VEGF-induced angiogenesis and lymphangiogenesis. *Nature.* 2010;465:483-6.
24.	Boucher P, Gotthardt M, Li WP, Anderson RG and Herz J. LRP: role in vascular wall integrity and protection from atherosclerosis. *Science.* 2003;300:329-32.
25.	Ibrahim S, Keating M, Do KA, O'Brien S, Huh YO, Jilani I, Lerner S, Kantarjian HM and Albitar M. CD38 expression as an important prognostic factor in B-cell chronic lymphocytic leukemia. *Blood.* 2001;98:181-6.

Deciphering the Epigenetic Code of Cardiac Myocyte Transcription

Sebastian Preissl, Martin Schwaderer, Alexandra Raulf, Michael Hesse, Björn A Grüning, Claudia Köbele, Rolf Backofen, Bernd K Fleischmann, Lutz Hein and Ralf Gilsbach

The online version of this article, along with updated information and services, is located on the
World Wide Web at:

http://circres.ahajournals.org/content/early/2015/06/23/CIRCRESAHA.115.306337

Data Supplement (unedited) at:

http://circres.ahajournals.org/content/suppl/2015/06/23/CIRCRESAHA.115.306337.DC1.html

---

Permissions: Requests for permissions to reproduce figures, tables, or portions of articles originally published in
Circulation Research can be obtained via RightsLink, a service of the Copyright Clearance Center, not the Editorial
Office. Once the online version of the published article for which permission is being requested is located, click
Request Permissions in the middle column of the Web page under Services. Further information about this process is
available in the Permissions and Rights Question and Answer document.

Reprints: Information about reprints can be found online at:
http://www.lww.com/reprints

Subscriptions: Information about subscribing to *Circulation Research* is online at:
http://circres.ahajournals.org//subscriptions/